

**Application of Electrical Resistivity and
Electromagnetic Prospecting Methods for Ground
water Studies around Dembi near Debrezeit**

**A thesis presented to the School of Graduate Studies of
Addis Ababa University
in partial fulfillment of the requirement of the degree Master of
Science
in Applied Geophysics**

By

Ewenet GashawBeza

**Addis Ababa
1998**

**Addis Ababa university
school of graduate studies**

**Application of Electrical Resistivity and
Electromagnetic Prospecting Methods for Ground
water Studies Around Dembi near Debrezeit**

Ewenet GashawBeza

June,1998

CONTENTS

	PA GE
ABSTRACT	III
ACKNOWLEDGEMENT	V
CHAPTER ONE	
1. INTRODUCTION	1
1.1 Purpose and overview of the study	1
1.2 Water bearing formations and ground water occurrence	4
1.3 Geological frame work of the area	6
Hydrogeology of the study area	8
1.4 Occurrence of ground water in igneous rocks	10
CHAPTER TWO	
2. ELECTRICAL RESISTIVITY METHODS	
2.1 Theory	12
2.1.1 Geoelectrical method	
2.1.2 The principle of equivalence and suppression	17
2.1.3 Resistivities of rocks and minerals	18
2.1.4 Electrode arrangement and field procedures	19
2.1.5 Depth of investigation	25
2.2 Data acquisition	26
2.3 Data processing and interpretation	27
2.3.1 Auxiliary point method	28
2.3.2 Inversion	28
2.3.3 The computer program	31
2.3.4 Final model parameters	32
2.4 RESULTS AND DISCUSSION	
2.4.1 Geoelectrical sections	33
2.4.2 Pseudosections	43
2.4.3 Apparent resistivity contour	51
2.4.4 Electrical profiling	58

CHAPTER 3	
3. ELECTROMAGNETIC METHOD	71
3.1 Theory	72
3.2 Description of EM fields	76
3.2.1 System descriptions	76
3.2.2 Depth of penetration	77
3.3 EM field procedures	77
3.3.1 The moving source method	78
3.3.2 GENIE	79
3.4 Data acquisition	81
3.5 Field results	82
3.6 Data interpretation	83
CHAPTER 4	
Summary and conclusions	89
References	

ABSTRACT

Combined electrical resistivity and electromagnetic prospecting methods were carried out around Dembi area near Debrezeit town. The analysis of the results obtained from both geophysical methods has provided useful information regarding the electrical characteristics of the subsurface which is related with the thickness and depth ranges of layers. The physical property distribution which is obtained by the two methods is analyzed with particular significance for ground water.

Twenty vertical electrical sounding (VES) measurements using Schlumberger configuration along four parallel profiles were conducted. The field apparent resistivity data is plotted against electrode separation and initial model parameters for each sounding station is obtained using auxiliary point method and two layer master curves. For quantitative evaluation of the resistivity soundings, the field data was submitted to a curve matching computer program. In this program the apparent resistivities obtained as a function of electrode spacings is converted to true resistivities as function of depth.

As result of inversion, a four layer geoelectric section is constructed for all profiles in the studied area. The investigation has made it possible to establish the layer stratification along all the profiles. Generally, this geophysical investigation around Dembi area has indicated a four layer earth structure.

The first layer is described by a more or less uniform thin layer of alluvial deposits. Underlying the top layer is a second layer characterized by a very low apparent resistivity value which represented the bottom part of the soil section with considerable moisture and clay content. The third geoelectric layer is made up of a vast portion of weathered and fractured basalt section which is assumed to be the most favorable site for the accumulation of subsurface water. From hydrogeological point of view, this layer satisfies the physical condition to be favorable host for ground water. Underlying the third layer a section identified by comparatively low apparent resistivity value is interpreted to be highly saturated volcanic ash and clay.

It was also possible to observe a generally decreasing apparent resistivity values towards the Western direction along each profile over the investigated area. A decreasing trend of apparent resistivity values were also observed due to the conductive nature of the ground towards North.

The results obtained from electromagnetic interpretation also showed anomalously high conductivity responses around the third and the fourth profiles. An increasing tendency of conductivity was also observed towards the Western direction coinciding with the result obtained from the resistivity survey.

The results of both geophysical methods has shown strong correlation in that, a decrease in apparent resistivity values in the sounding survey is associated with an increase in electrical conductivity obtained from electromagnetic survey towards North and West of the studied area.

ACKNOWLEDGEMENT

I Gratefully acknowledge the continuous advice and encouragement rendered by my advisor and instructor Dr. Tigistu Haile who devoted much of his time and energy at all stages of this research work.

My sincere appreciation also goes to My co-advisor Ato shimeles Fisseha, a very cooperative person, who most happily forwarded me important ideas from the vast reservoir of his practical experience.

My thanks are due to my father Ato gashawbeza Mengesha, who took my earliest footsteps in the paths of knowledge and also my mother W/o Bayush Nicola who always wish best for her son. Special thanks are also due to my elder brother Ato Bemnet Gashawbeza whose acadamic excellence have been found to be of cardinal importance for my determination to follow his ways and arrive at this stage.

It is a pleasure to thank my heartily brother Ato Tegene Asfaw and helpful friends Ato Tewodros Getachew and Alemayehu Berehie for their constant moral support which I found it to be valuable for my success. Sincere appreciation also goes to W/o Yewubnesh Tezera and her family. I am particularly indebted to Ato Yalemwork Tezera who showed considerable concern and interest during the data acquisition in the field.

I am also grateful to the department and staff members of EIGS for providing processing facilities and library resources. Finally, I would like to thank the school of graduate studies of Addis Ababa University and the department of Geology and Geophysics for financial support for the project and providing geophysical equipment and laboratory facilities.

to fulfill the increasing demand which has resulted from increased population and improved way of living. Therefore, with the increasing shortage of available clean water, it becomes essential to supplement these water supplies with other sources and one of these is ground water.

With the projected increase in population over the country including the major and intermediate cities/towns, it is time to carry out a thorough ground water potential assessment and studies for most growing towns.

Debre Zeit, which is located about 45 km east of Addis Ababa is one of the fast growing cities in Ethiopia. The existing water supply schemes are not able to meet the demand of the growing population, and industries. As the demand increases, the quantity and quality of the available supply is not expected to meet the demand. Therefore, it is high time that an exhaustive study on the promising potential areas for future ground water development to be carried out.

In the past, water wells were sited at random and this often lead to disappointing results even when the locations were based on previous trials. To avoid drilling wells in unfavorable locations, a reliable method is required for assessing formation parameters before drilling takes place. This may ensure that the prospective production wells be sited where the aquifer is of adequate yield and the water is of good quality.

Geophysics is guided by the intellectual curiosity about the nature of the earth and also the more secular need to know what resources and materials are available to mankind, where and in what quantities. A geophysicist is required to prepare a geological map at depth by measuring the physical fields on the ground, in the

mines, in bore holes, in space, etc. Scientific instruments measure changes in physical properties of rocks which are concealed beneath the surface.

For instance, change in density of rocks will cause minute changes in the gravitational field, magnetic rocks will produce disturbances in the earth's magnetic field, conductive rocks will affect ground response to artificially stimulated electric fields etc. Each of these phenomena involve the disturbance of normal or predictable state of affairs by an addition of local perturbations which are called anomalies. Physical fields which are available for such investigations are seismic wave field, gravity, magnetic, geoelectrical, electromagnetic, natural radioactivity fields, etc.

The characteristics of various fields are governed by the properties of the medium they interact with as well as the properties of source they generate. It is these Characteristics imparted by the medium properties that are of interest for exploration geophysics which strives for mapping the earth's interior. The present thesis deals with application of the above principles specially for hydrogeological studies.

The choice of a geophysical method will depend on which physical properties of the geological formations or structures have the greatest contrasts. The four main physical properties whose contrasts are detected by the geophysical methods are electrical resistivity, seismic velocity, magnetization and density.

In this regard, the aim of this thesis research are to evaluate the application of geophysical methods to interpret the data with the following objectives;

1. To delineate the most promising areas for future ground water development by studying the kind and thickness of the overlying strata and the lithology encountered with it,
 2. To study the occurrence and distribution of ground water bearing formation,
 3. To study the location of and depth to the water bearing formation,
 4. To verify the occurrence of important ground water reservoirs with in unconfined, semi-confined and confined aquifers which are suggested to exist in the area (Tamiru , 1992),
 5. Delineating tectonic and structural features which may serve as conduits for ground water flow in to or out of the aquifers,
 6. To examine the extent of effectiveness of the combined geophysical methods which are employed in the investigation, and
- the specific objectives include;
1. Determining the general resistivity stratification of the area,
 2. Locating sites favorable for sufficient and sustainable yield of ground water, and
 3. Getting structural and lithological information by the combined geophysical methods which are employed.

1.2 Water bearing formations and ground water occurrence

The mode of ground water occurrence are affected by the geologic development and properties, delineation, and boundary conditions of soil and rock formations

through which the water percolates. They depend also on ongoing activities and climatic and environmental conditions. These formations may be extensive or limited between natural or artificial boundaries. The degree of water productivity depends on the degree of natural water recharge, its physical and chemical properties, climatic conditions, the characteristics of its geometric and hydrologic boundaries etc.

The amount of water which a rock holds depends on its porosity. This is the proportion of the volume of rock which consists of pores, and it is usually expressed as percentage. The principal factors which affect porosity are grain size and shape, and the degree of sorting in an consolidated sediments. Those sediments which have been ideally sorted and have rounded grains of uniform size are the most porous. Porosity decreases as the angularity of the grains increases, because the grains pack together more closely. Similarly, as the degree of sorting is reduced smaller grains fill pore spaces between the larger grains and porosity is also reduced.

In consolidated rocks, porosity tends to be lower than in unconsolidated sediments, because part of the pore space is taken up with cement. Some rocks with relatively high porosity values may be poor transmitters of water because individual pores are not interconnected. (Brassington, 1990)

1.3 Regional geologic setting and Geological framework of the area

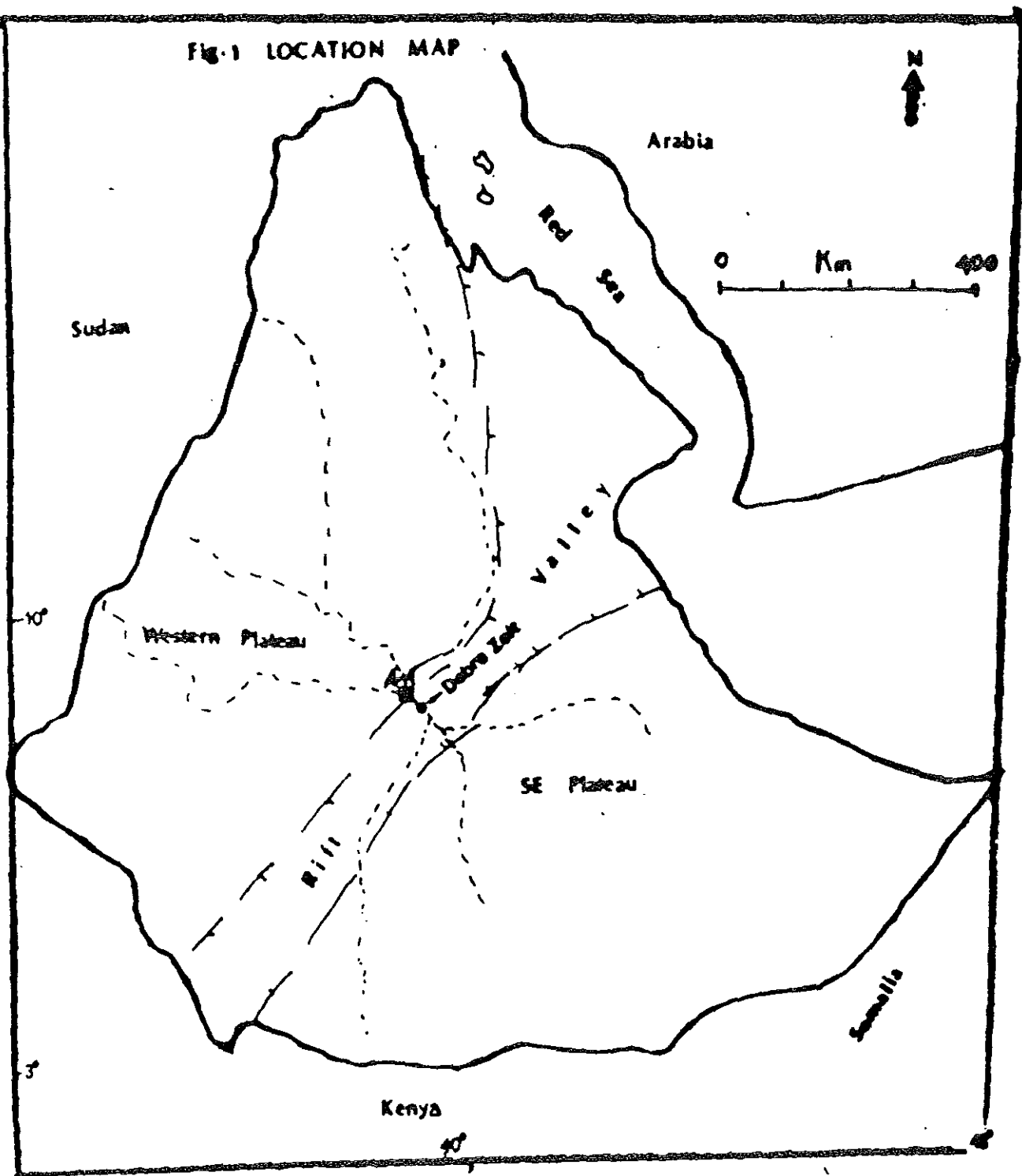
The studied area is located on the western margin of the Main Ethiopian rift . The rift system which forms the main Ethiopian rift is one of the latest structural features of the earth's crust being also related to the rift valley pattern of east Africa.

The volcanic rocks related to the rift have been out poured after the formation of the rift, when fissural volcanism in the related plateau had died out(Zenatin et al. 1980). In Ethiopian rift basalts and rhyolites are the predominant rocks with some intercalations of trachytes and pyroclastics. From Addis Abeba down to the rift floor at Mojo, a great number of NE-SW faults occur upthrown NW, the most important being the Dukem fault (Mohr,1967) which is close to the studied area.

According to Mohr, the basal rocks in Debrezeit region are probably constituted by trap series basaltic lavas even if not exposed in the vicinity of the area , being covered by more recent thick lavas, tuffs and lacustrine sediments. Extensive pliocene - quaternary volcanicity characteristics of most of the Ethiopian rift is also conspicuous in this region The geomorphology is typically that of a volcanic area and is slightly modified by the deposition of lacustrine sediments during the pluvial period(Tesfaye cherenet).

In the area under investigation the following lithologic units have been identified; rhyolytic flows, rhyolytic ignimbrites, olvine basaltic flows,basaltic cyndercones, surge deposits, ash flows and alluvial sediments. While the mafic volcanic rocks are mainly dominated by basaltic cynder cones and olvine basaltic lava flows, the acidic ones are

Fig. 1 LOCATION MAP



7

3

dominated by rhyolitic lava flows and surge deposits with only small out crops of trachytic domes. In the area, fractures and faults are mainly aligned in the north east direction(Tamiru ,1992).

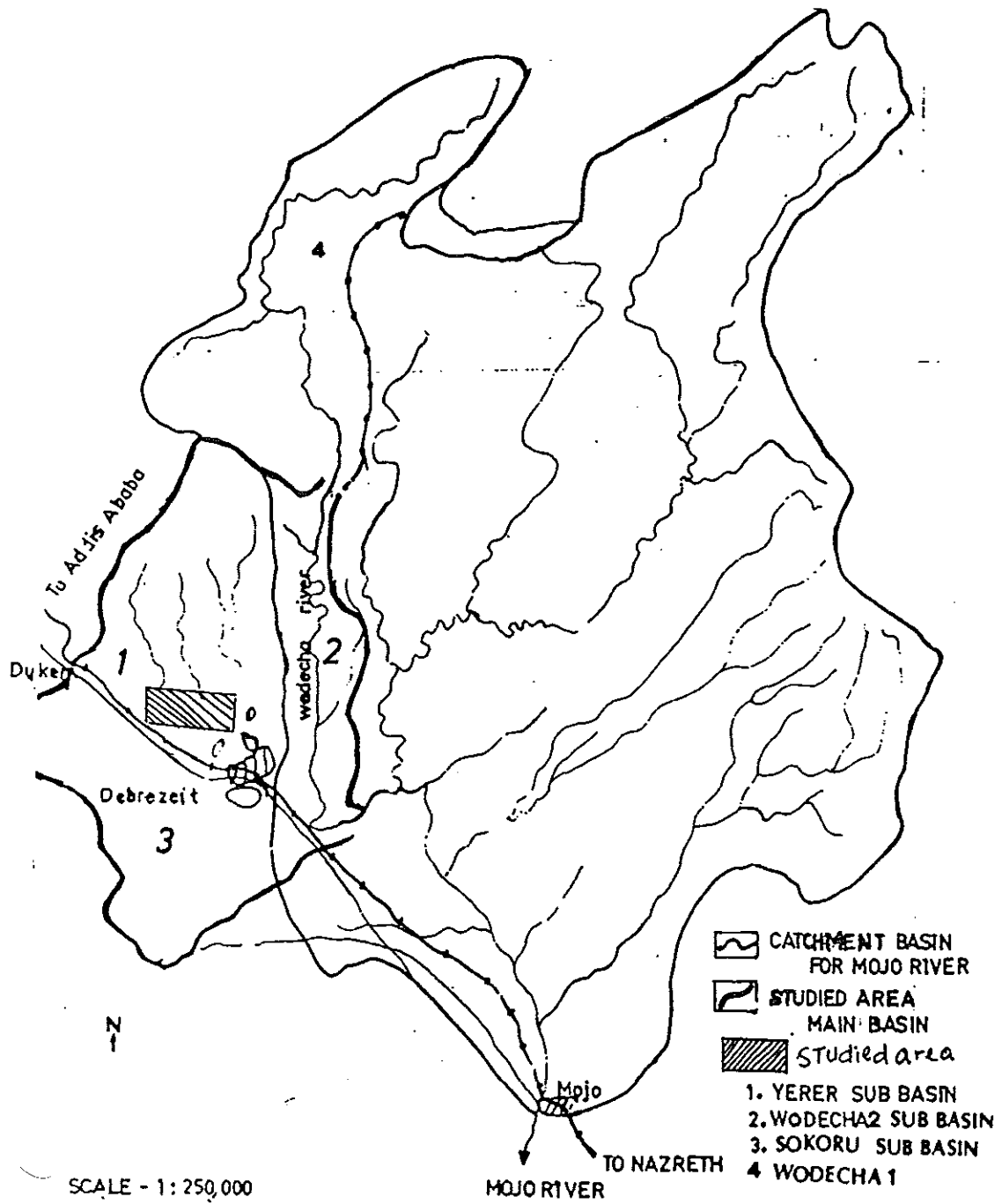
Lithological log in adjacent area shows silty clay cover underlain by vast section of weathered olvine and scoriaceous basalt extending up to a depth of 72 m. The bottom section of the log is volcanic ash and silty clay.

Hydrogeology of the studied area

The cover of the plane area is dominated by clay and silty soils. The alluvial sediments are mainly exposed along the gullies of the intermittent streams. Despite the lateral variability, the unit shows, a regular vertical sequence From coarse sand at the bottom to clay at the top. Generally these sediments are very loose so that they can be eroded away.

In the Northern and Western part of the studied area, runoff occurs from a relatively impervious portions of highly elevated part of the area which passes over a more pervious soil and is partly or completely absorbed before reaching the flat area near Debrezeit. In the rainy seasons, there is also appreciable ponding or surface storage for long period of time, and this creates an opportunity for infiltration to occur. This might have resulted because the topography is flat and due to clayey nature of the cover soil. According to hydrological studies conducted over the area, the multi layer aquifer in the Yerer sub basin is fed by the run off coming from the well developed drainage pattern of Mt. Yerer and by the direct infiltration of the rain water when black clayey top soil is absent or affected by evident shrinking cracks which allow percolation of water. (Tamiru ,1992)

STUDIED AREA & MOJO RIVER CATCHMENT BASIN



1.4 Occurrence of ground water in igneous rocks

Because the studied area is made up of mainly igneous it is important to see ground water occurrence in relation with such rock types. The dominant volcanic rocks in the earth's crust are basalts, andesites, trachytes, dacites, rhyolites and pyroclastic rocks such as welded tuffs (ignimbrites), un welded tuff surge deposits, pumice and scoria. Ground water occurrence in such areas is the major water supply for large part of the world since they have significant hydrogeological characteristics important to ground water movement and storage.

The ground water circulation and storage capacity of volcanic rocks depend on the nature of the porosity and permeability of the aquifers. Taking into consideration the physical nature of the flows and the environment in which the lava is cooled the permeability of such fresh rocks making up an aquifer is generally high.

The most important features governing the ground water flow and storage in volcanic rocks are, vertical permeability due to primary and secondary fractures or horizontal permeability or due to horizons containing opening due to the lava flow and gas expansion during solidification or due to occurrence of impervious horizons and dykes. In the volcanic terrain, it is possible to find potential water bearing zones interceded with relatively impervious units. In such aquifers ground water occurs under confined conditions. Interbedding of massive units with fractured and porous media also gives rise to multi-layer aquifer systems.

Volcanic rocks are characterized by a high range of porosity and permeability variations from highly permeable basalts to highly porous but quite impermeable pyroclastics. In volcanic rocks, the occurrence of water bearing structures is

conditioned by the primary and secondary porosity and permeability of the lithological units, but all rock structures possessing a primary porosity may not have a primary permeability. But their latter connection by means of weathering or fracturing may give rise to a secondary permeability.

CHAPTER TWO

ELECTRICAL RESISTIVITY METHODS

GENERAL CONSIDERATIONS

The rocks of earth's crust vary in their physical properties such as density magnetism, rigidity, compressibility, etc. Geophysics is the application of the principles of physics to the study of the above properties of the earth and its internal constitution from the physical phenomena associated with it. This is attained by using suitable instruments at the earth's surface, with which some of the significant variations in the physical properties (anomalies) can be detected and the results can be interpreted to give information concerning the distribution and arrangements of certain types of rocks at deeper levels inside the earth.

2.1 THEORY

2.1.1 GEOELECTRICAL METHOD

Introduction

Geoelectrical exploration is a major branch of exploration geophysics which makes use of a large variety of techniques each based on some different electrical characteristics of materials in the earth. Of these different geophysical methods, the method employed on the studied area is electrical resistivity method.

The resistivity of rocks vary due to the differences arising not only from inherent characteristics of the rocks but also from their position with respect to the earth's surface and the amount of pore fluids contained in rocks. Since loose sediments,

gravels, sands and the like contain much water in their pores, and, are therefore much better conductors than the compact bed rocks on which they lie. Resistivity surveys are especially valuable in finding the thicknesses of such a cover on the bed rock.

In the electrical resistivity method, a direct, commutated or low frequency alternating current is introduced into the ground by means of two electrodes (iron stakes) connected to the terminals of a portable source of EMF. The procedure then is to measure potentials at other electrodes in the vicinity of current flow, the resulting potential distribution on the ground as measured by the inner potential electrodes is capable of yielding the distribution of electrical resistivity below the surface. This method has been used for searching water bearing formations or in stratigraphic correlation in oil fields and for prospecting conducting ore bodies.

The potential difference for unit current sent into the ground is the measure of electrical resistance of the ground between the measuring terminals. This resistance is a function of geometrical configuration of the electrodes and the electrical parameters of the ground.

The basic concept used to delineate subsurface geology through geoelectrical method is that electrical resistivity is a function of length taken either in the vertical or horizontal direction. In the field layout the electrodes are either expanded outwards about a center point which is known as vertical electric sounding (VES) or, on the other hand, the field lay out moves along a profile keeping a fixed distance between the electrodes, to study the lateral changes in electrical resistivity known as profiling.

In VES potential difference and multiplication of resistance with a suitable geometrical factor defined by the electrode layout determines a function known as apparent resistivity. From this measured apparent resistivity data, one can estimate the electrical parameters of subsurface geological formations, which are based on established physical laws. The physical principle underlying the resistivity method is embodied in ohm's law. The equation for electrical potential is obtained by applying the fundamental principle of conservation of charges which results in the Laplace equation for homogeneous and isotropic medium of constant resistivity as

$$\nabla^2 V = 0 \quad (1)$$

The resistivity determined would have been true resistivity if the ground were homogenous and isotropic. However, usually, the ground constitutes various materials and there may be some variations in the lateral or vertical dimensions and the resistivity determined is called apparent resistivity. The apparent resistivity measured depends not only on the nature of the geologic system but also on the geometric dispositions of the electrodes used for the measurement. The apparent resistivity is formal, rather artificial concept and should not be construed, in general as representing average resistivity of earth or any other similar thing. The artificiality will be evident from the fact that negative values are perfectly possible(Parasnis,1979)

The equation for the potential at the surface due to a point source of current I is obtained by solving eqn.(1) in spherical coordinate system (r,θ,ϕ) by taking complete symmetry of current flow with respect to θ and ϕ directions as,

$$V(r) = \frac{I\rho}{2\pi r} \quad (2)$$

From equation (2) an expression may be derived for apparent resistivity from potential difference between two measuring electrodes, the amount of current flowing I and the appropriate geometrical factor(k) for the measurement configuration as,

$$\rho = k \frac{\Delta V}{I} \quad (3)$$

One type of conductivity distribution that adequately describes many geological situations is that represented by an earth composed of several horizontal strata. This model is of particular interest in prospecting for ground water by resistivity methods and is outlined as follows. If an n -layered earth having resistivities ρ_i ($i=1,2,\dots,n$) and thicknesses d_i ($i=1,2,\dots,n-1$) is energized by a point current source emanating a current I placed at $A(0,0,0)$, Fig(3) .

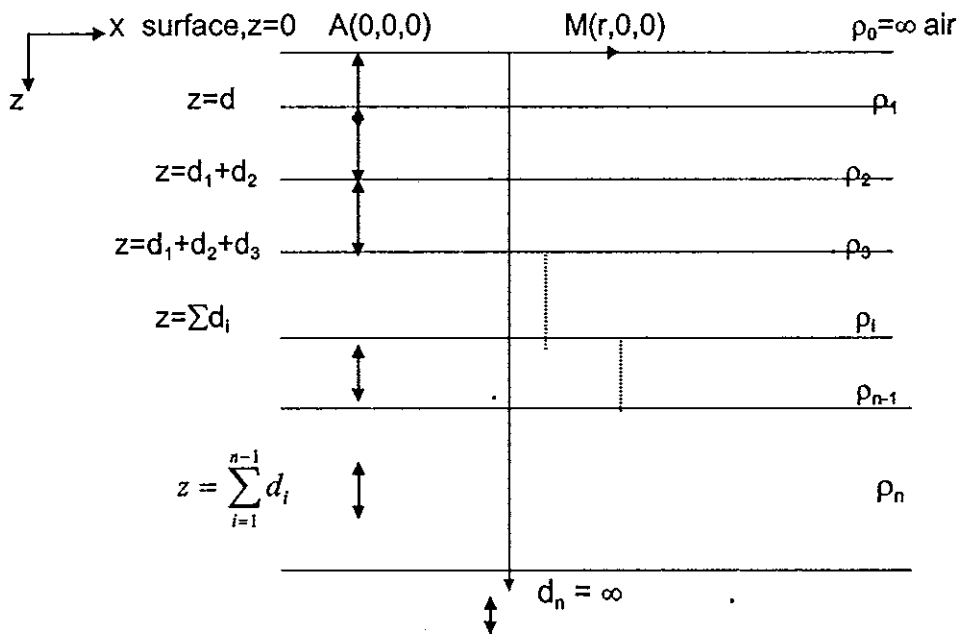


Fig (3) Horizontally stratified earth

Stefanescu has given an expression for the potential at an arbitrary point $M(r,0,0)$ on the surface as

$$V(r) = \frac{I\rho}{2\pi} \left[\frac{1}{r} + 2 \int K(\lambda) J_0(\lambda r) d\lambda \right] \quad (4)$$

where $J_0(\lambda r)$ is the Bessel function of first kind and zero order, and $k(\lambda)$ is resistivity kernel function, determined by resistivities and thicknesses of the layers, and may have all possible values ranging from -0.5 to ∞ (Israel,1994)

Equation(2) is the equation for the potential when only one measuring point is considered. However, for actual field work we need at least two current electrodes (source and sink) to complete the circuit and two measuring electrodes as one can measure only the potential difference between two points and not the absolute potential.

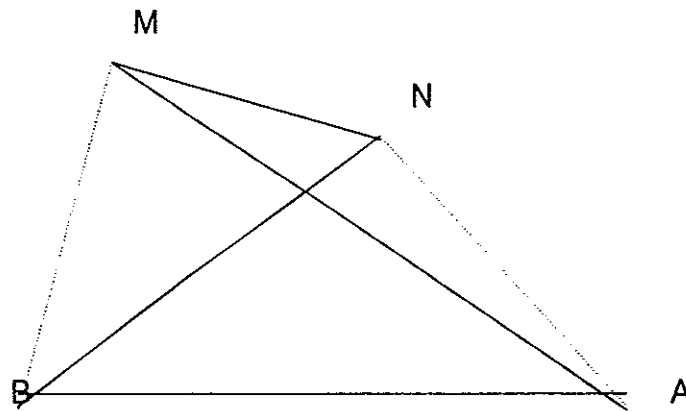


Fig. (4) General four electrode array

In a system of four electrodes comprising two current electrodes (A,B) and two potential electrodes (M,N) the expression for the apparent resistivity assuming the electrode separations as $AM=r_1$, $BM=r_2$, $AN=r_3$ and $BN=r_4$ is given by

$$\rho_a = 2\pi \left[\frac{\rho_1 \rho_2 \rho_3 \rho_4}{\rho_2 \rho_3 \rho_4 - \rho_1 \rho_3 \rho_4 - \rho_1 \rho_2 \rho_3 + \rho_1 \rho_2 \rho_3} \right] \frac{V_m - V_n}{I} \quad (5)$$

2.1.2 The principles of equivalence and suppression

In actual applications of various interpretation methods to a particular field problem, limitations are set by maximum distance from the current source to which the electric field is given, and by the irregularities in the field due to surface non homogeneities. Further more, all measurements have finite accuracy. On account of all these causes, widely different resistivity distributions may lead to apparent resistivity curves which, although they are not identical, can not be distinguished in practice. This introduces ambiguity in the interpretation.

Mathematical formulation of two simple types of equivalence can be easily obtained. If we consider, for example, a relatively thin layer sand witched between two layers whose resistivities are much larger than the sand witched layer. Then the current flow in the earth will then tend to concentrate into the middle layer Fig(5a). The resistance of the elementary block of length ΔL , and cross section, $h \Delta m$, to such a current flow is

$$R = \frac{\rho \Delta l}{h \Delta m} \quad (5)$$

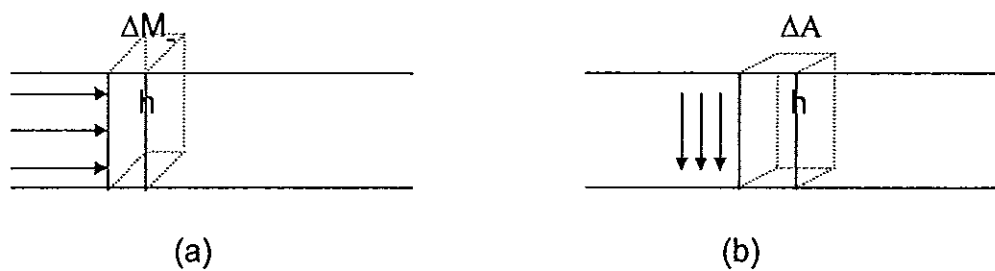
and this will be unaltered if we increase ρ and at the same time increase h in the same proportion. Thus all such middle layers for which the ratio h/ρ is the same are electrically equivalent.

On the other hand, if the resistivity of the middle layer is much larger than that of the layers on either side of the middle layer, the electric current will tend to avoid it

and take the shortest route to the lower layer. The lines of the current flow will be almost perpendicular to the layer Fig(5b). The resistance of the elementary block will be,

$$R = \frac{\rho h}{\Delta A} \quad (6)$$

where, ΔA is the cross section. In this case, all layers for which the product hp is the same are electrically equivalent so that, h , and ρ can not be determined uniquely Fig.(5) (Parasnis,1979)



Fig(5) The principle of equivalence

2.1.3 Resistivities of rocks and minerals

In most rock materials the porosity and chemical content of the water filling the pore spaces is more important in governing resistivity than the conductivity of the mineral grains of which the rock itself is composed. When the pores are saturated with fluids it will be governed by the fluid resistivity. The salinity of the water in the pores is probably the most critical factor determining resistivity. But when there are porous rocks, particularly those with large concentrations of magnetite or

graphite lying above the water table at shallow depth or, when they occur at such great depth that all pore spaces are closed by ambient pressure, the conduction through them will be with the mineral grains themselves. Under these conditions, the resistivity of the rock depends on the resistivity of the grains. When the pores are saturated with fluids it will be governed by the fluid resistivity.

The range of resistivities among rocks and minerals is enormous, extending from 10^{-5} to $10^{15} \Omega \text{ m}$. Rocks and minerals with resistivities from 10^{-5} to $10^{-1} \Omega \text{ m}$ are considered to be good conductors, while those from 1 to 10^7 are intermediate, and those from 10^8 to 10^{15} are poor conductors.

There is no consistent difference between the range of resistivities of igneous, and sedimentary rocks, although metamorphic rocks appear to have higher resistivity. There is also effect of geologic age upon the resistivity of rocks. Normally, one should expect a fairly uniform increase of resistivity with geological age because of the greater compaction associated with increasing thickness of overburden. But the anomalously high resistivities of tertiary rocks reflect the fact that the deposition at this time was, mainly on fresh water than in salt water as was the case during Mesozoic (Dobrin, 1976).

2.1.4 Electrode arrangement and field procedures

The selection of a particular electrode array for resistivity survey is controlled by many variables, perhaps the most important being the strength of the anomalous response of the arrays over the type of target which is being sought. Other considerations which may influence the choice of an electrode array in a survey are, the purpose of the project, the speed of coverage, the terrain, the power and sensitivity of the instrument, the ground current noise, the ease of interpretation of

the data for that particular array, the number of personnel available, the resistivity of the ground etc.

Every electrode array has its advantage and drawbacks depending on the conditions. The best choice of the array requires a careful consideration of the condition of each individual survey(Saydam and Duck worth, 1978).

In actual practice a number of different surface configurations are used for current and potential electrodes. In most arrangements both sets of electrodes are placed on the outside of the potential electrodes although the opposite arrangement should in principle be equivalent. The potential difference at any point due to the current flow is equal to the sum of the contributions from the individual current electrodes .The potential difference measured in a four electrode survey over a homogenous ground is given by ;

$$\Delta V = \frac{I\rho}{2\pi} \left[\frac{1}{r_1} - \frac{1}{r_2} - \frac{1}{r_3} + \frac{1}{r_4} \right] \quad (7)$$

Three of the most widely used configurations are Wenner , Schlumberger, and Dipole-Dipole arrangements.

1. The Wenner arrangement

It is one of the most common electrode arrangements for resistivity measurement. Here, each potential electrode is separated from the other adjacent current electrode by a distance "a" which is one third the separation of the current electrodes.

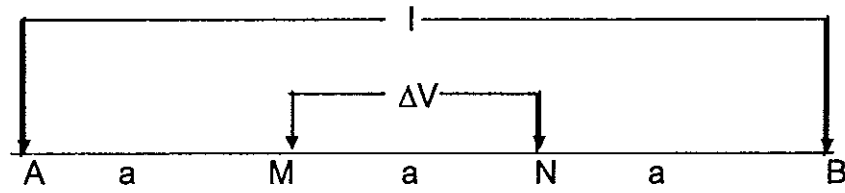


Fig (6) The Wenner configuration

applying eqn.(7) for this geometry we get,

$$\Delta V = \frac{I\rho}{2\pi} \left[\frac{1}{a} - \frac{1}{2a} - \frac{1}{2a} + \frac{1}{2a} \right]$$

$$\Delta V = \frac{I\rho}{2\pi} \left(\frac{2}{a} - \frac{1}{a} \right)$$

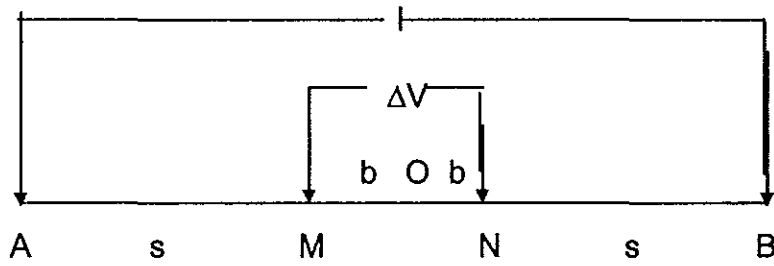
$$\Delta V = \frac{I\rho}{2\pi a} \quad \text{or,}$$

$$\rho = 2\pi a \left(\frac{\Delta V}{I} \right) \quad (8)$$

For depth exploration using Wenner array, the electrodes are expanded about a fixed center and increasing the spacing "a". Depth sounding using Wenner array is inconvenient in the field, but, for lateral exploration or mapping, the spacing remains constant and all the four electrodes are moved along the line and it is better for field work.

2. The Schlumberger spread

In Schlumberger configuration, the operator expands the electrode spacing by increasing the distance between current electrodes or that between potential electrodes, but one at a time during the course of measurement.



Fig(7) The Schlumberger configuration

$$r_1 = AM = s - b$$

$$r_2 = BM = s + b$$

$$r_3 = AN = s + b$$

$$r_4 = BN = s - b, \text{ so that, eqn.(7) for schlumberger}$$

configuration becomes;

$$\Delta V = \frac{I\rho}{2\pi} \left[\frac{1}{s-b} - \frac{1}{s+b} - \frac{1}{s+b} + \frac{1}{s-b} \right]$$

$$\Delta V = \frac{I\rho}{2\pi} \left(\frac{2}{s-b} - \frac{1}{s+b} \right)$$

$$\Delta V = \frac{I\rho}{2\pi} \left(\frac{2b}{s^2 - b^2} \right)$$

$$\rho_s = \pi \left(\frac{s^2 - b^2}{2b} \right) \frac{\Delta V}{I} \quad (9)$$

or, it can be expressed as function of the distances between current and potential electrodes as

$$\rho_a = \pi \left[\frac{(AB)^2 - (MN)^2}{MN} \right] \left(\frac{\Delta V}{I} \right) \quad (10)$$

Though site selection is very important in all sounding work it is particularly critical with Schlumberger array, which is very sensitive to conditions if directions of

expansion are often constrained by topography. The outer electrodes of Schlumberger array are usually moved in steps which are approximately logarithmic while taking measurements. When, eventually, the voltage drop becomes too small to be accurately measured then the inner electrodes then must be moved further. Overlap readings are taken at places where the potential electrode positions are changed.

3. Dipole- dipole method

Dipole-dipole array is another class of resistivity sounding array. In this of configuration there are several patterns of expansion of current and potential electrodes. One of the commonly utilized configuration is the polar dipole-dipole configuration. In this array MN are outside of A,B and of the same line, each pair having a mutual separation "a", if "na" is the distance between the two inner most electrodes B,M, then

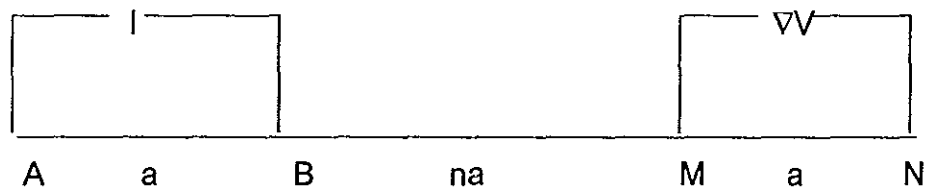


Fig (8) dipole dipole array

$$\rho_a = K \frac{\Delta V}{I},$$

where

$$K=2\pi \left[\frac{1}{AM} - \frac{1}{BM} - \frac{1}{AN} + \frac{1}{BN} \right]$$

is the geometrical factor.

From geometry of the figure, $AM=a(n+1)$, $BM=na$, $AN=a(n+2)$, $BN=a(n+1)$. After substitution and rearrangement this expression reduces to

$$\rho_a = \pi n(n+1)(n+2)a \left(\frac{\Delta V}{I} \right) \quad (11)$$

The advantages of dipole dipole array is that the distance between the current source and the voltage receiver systems can be increased indefinitely, being subject only to instrument sensitivity and noise. The increase of electrode separation in Wenner and Schlumberger arrays is limited by cable length.

Regardless of the specific electrode spread employed, there are really only two basic procedures in resistivity work. The particular procedure to be used depends on whether one is interested in resistivity variations with depth or with lateral extent. The first is called electric drilling, and the second electric mapping or trenching.

Electric Drilling

Since the fraction of total current which flows at depth varies with the current electrode separation, the field procedure is to use a fixed center with expanding spread. The Wenner and Schlumberger layout are particularly suited for this purpose. The presence of horizontal or gently dipping beds of different resistivities are best detected by expanding spread. Hence, this method is useful in determining the depth of overburden, depth, structure and resistivity of flat lying sedimentary beds and possibly the basement also if it is not too deep (Telford, 1976).

Electric Mapping

This method is particularly useful in mineral exploration where the detection of isolated bodies of anomalous resistivity is required. The method is also useful for detection of vertical discontinuities and identification of weak zones. Again the two commonly used layouts are Wenner and Schlumberger. In all such cases the apparent resistivity is plotted at the mid point of the potential electrodes.

2.1.5 Depth of investigation

Depth of investigation is an important physical concept in any method of geophysical prospecting. For fields describing signals that propagate, depth of investigation has a quite precise and clear meaning.

In many of the artificial field methods, the contributions from the various earth layers at increasing depths do not fall off monotonically with increase in depth but pass through a maximum. Then we can define depth of investigation unambiguously as that depth which contributes most to the total signal measured on the ground surface. It does not mean that the entire measured signal originate at that depth alone. Contributions to the observed signal may come from all depths, but the contribution from the depth of investigation is the largest. In that case, our depth of investigation is synonymous with the depth of maximum contribution of signal. Since potential values consist of contributions from all depths, the maximum contribution depends on

1. The number of layers contributing significantly,
2. Layer resistivities and thicknesses and

3. Electrode configurations and separations

But, there is no simple rule and simple empirical relations that can take care of resistivity, depth and electrode separations, but it is considered as a rule of thumb that $1/3^{\text{rd}}$ to $1/4^{\text{th}}$ of the electrode separation in Schulumberger array equals to the depth of investigation (Frolich, 1967).

2.2 Data acquisition

In the present work, for the electrical survey, the field layout is conveniently chosen and the survey grid is divided into four equal parallel profiles each having separation of 500 meters. Five sounding stations along each profiles are chosen with spacing of 200 meters. Then electrodes are inserted to the ground and measurements are taken under a predetermined current electrode separations which are approximately logarithmic. The amount of current injected by the current electrodes is measured by the TSQ-3 square wave transmitter which is supplied by power from ac generator (Briggs-straton). The resulting potential difference is measured by IPR-8 receiver which is connected to the potential electrodes. The apparent resistivity value is calculated by using eqn.10 and the measured apparent resistivity is plotted against $AB/2$ on a logarithmic paper right after each measurement to observe the curve trend on the field which is very helpful to correct out liars which are introduced by measurement errors and repeat observations if necessary before it is too late.

Twenty VES are made using Schulumberger field array with spacing between successive VES stations 200m, along four parallel profiles directed NW-SE. The

Schulumberger method is chosen because it is proved to be effective for exploration of deep or thick sediments (A chessman et al, 1976). In our study the variation of conductivity is assumed to be in vertical direction since in areas of flat and laterally undisturbed geology as in sedimentary basins, the vertical is the preferred direction of electrical conductivity change. In this method a pulsed ac current is introduced into the ground through two outer current electrodes A and B. The resulting potential is measured between two closely spaced inner electrodes M and N located at the center of the sounding.

Measurements are made at increasing current electrode spacing and the apparent resistivity is calculated using the relation,

$$\rho_a = K \frac{\Delta V}{I}$$

Then the sounding curves are plotted using the values of apparent resistivity vs AB/2 of the Schulumberger expanding spread.

2.3 Data processing and interpretation

The aim of interpretation of resistivity sounding data is to determine the thickness and resistivity of the different horizons from studying of the resulting field curves and the use of these results to obtain geological picture of the area under investigation.

Therefore, the first step towards the interpretation involves, plotting the apparent resistivity data against AB/2 on a transparent double logarithmic paper with the same modulus (62.5mm) as the existing theoretical master curves. Then keeping

the axes parallel, the transparent paper is slid on various master curves in succession until a satisfactory match is obtained with some curve. In case if there is perfect coincidence of the theoretical curve with the field curve, then the values of the field parameters are the same as those layer parameters for which the theoretical curves are constructed. But, it is, however, practically impossible to have an album of theoretical master curves representing all geological situations met in the field. Books of three layer master curves are available but a full set of four layer master curves will fill a small room(Wilson,1995). It is this problem which necessitated the need for devising ways of interpreting the observed field curves with the help of a limited number of theoretical curves available.

2.3.1 Auxiliary point method

This method is very important, in that it can be used to interpret, in principle, any number of layers by alternate use of two layer master curves, which is done by matching the initial branch of the field curve with an appropriate two layer master curve and a family of auxiliary point curves that correspond to the field curve type. Therefore, rough estimation based on segment by segment matching will be the best that can be done. The process is controlled by using those auxiliary curves to define allowable positions of the origins of the two layer curve being fitted to the latter segments of the field curve. The first approximation of the layer parameters were thus obtained through the above method.

2.3.2 INVERSION-

Introduction

Geophysical inversion involves the estimation of the parameters of a postulated earth model from a set of observations. Inverse theory is an organized set of mathematical techniques for reducing data based on inferences drawn from observations. The role of inverse theory is to provide information about the model parameters starting with data and general principle. Therefore, the basic statement of an inverse problem is that the model parameters and the data are in some way related and that relationship is known as the model.

A model response can be either a linear or nonlinear function of the model parameters. The inversion of VES data is nonlinear inversion and hence the determination of the model parameters involves iterative procedures which employ an approach of modifying the parameters of an initially guessed model which are used to compute a new model response estimate. At each stage, the sum of the squares of the error between the model response and the observation values is monitored. The iterative search for the parameters estimates terminates whenever either the squared error or the relative squared error becomes less than the pre specified value.

Iterative procedure

This approach can be employed if the relationship between the data and the model parameters is purely nonlinear. This relation between the model parameters and the data can be expressed in functional form as ;

$$F(m) = d \quad (12)$$

The standard procedure to solve such a case is to linearize the problem and iteratively impose guesses of m . The linearization involves expanding $F(m)$ in Taylor's series about m^0 which yields ,

$$F_i(M^0 + \delta m^0) = F_i(m^0) + \left. \frac{\partial F_i}{\partial m_j} \right|_{m=m^0} \delta m_j + \text{higher order terms} \quad (13)$$

neglecting the higher order terms from Eqn.(13) and rearranging yields:

$$\left. \frac{\partial F_i}{\partial m_j} \right|_{m=m^0} \delta m_j = d_i - F_i(m^0) = \delta d_i \quad (14)$$

Assuming the derivative evaluated at the guessed solution as,

$$\left. \frac{\partial F_i}{\partial m_j} \right| = G_{ij} \quad (15)$$

substituting Eqn.(15) in Eqn.(14) yields

$$G_{ij} \delta m_j = \delta d_i \quad \text{or} \\ \Delta d = G \Delta m \quad (16)$$

It is important to note that the relation in (16) is not linear with respect to the model parameters and the data themselves, but rather the linearity is with respect to the changes in the model and the data. The least squares solution for linear inverse problems is given by,

$$M^{est} = (G^T G)^{-1} G^T d. \quad (17)$$

From equation (17) it is possible to observe that the existence and stability of the solution depends on the existence of $(G^T G)^{-1}$. If eigen values are very small then the inversion is not stable and if some of the eigen values are zero the solution

does not exist. To overcome this problem the following modification is developed instead of equation (17) for nonlinear inversion as given by Marquadt (1970)

$$\Delta M^{est} = (G^T G + KI)^{-1} G^T \Delta d \quad (18)$$

Equation(18) is the Ridge regression approach for solving nonlinear inverse problems. In this equation, K, is the damping factor and I is an identity matrix . To have stable solutions the choice of K is very important. For K =0 the regression method reduces to the usual least squares method. Usually, K is chosen to take values ranging from 0.1 to 10.

In general, the damping factor, K, for the geophysical data can be determined from the G matrix .The appriori estimate for K is computed as,

$$K = [\sum \sum (G_{ij})^2]^{1/2} \quad (19)$$

where, the summation goes up to M and N which are the dimensions of the G matrix. Using first, the value of K from (19), the inversion is performed to obtain the new model. Then, the error between the observed and the predicted is cheked and if the error is not decreasing then K, is doubled and the computation is performed again and again until the error decreases up to an acceptable limit.

2.3.3 The computer program

The computer program used in this work for the determination of the final model parameters is Resist 87. What is actually going on in the program is briefly outlined bellow

- first array type used in the data collection is specified and the field data for each sounding station is loaded along with the current electrode spacing. This is done for all sounding stations
- before processing, the program asks for the data file that contains the apparent resistivity values from which the initial model parameters have been approximated. This makes the program ready for comparison of the assumed model parameters and the field curve
- then, it asks instructions to specify noisy data, etc.
- when choosing the model entering option, the program inquires for the number of layers, resistivity, and thicknesses assumed for the initial guess. The program requires the values to be given in order and starting from the first layer.
- after the required inputs as specified above are supplied, the program displays the graph of the field curve with the model given in step above.
- then, it asks instructions for specifying the root mean square error limit allowed for the iteration procedure to terminate and becomes ready for iteration
- the iteration continues as commanded by the user until the calculated error becomes less than the prescribed error limit .

2.3.4 Final model parameters

As seen from the previous discussions, the layer parameters thus obtained by curve matching are fed to the computer as an initial guess and the inversion process undergoes a number of iterations, as described above, to obtain more accurate models that give best fit in the sense of least squares.

The number of iterations required depends on the quality of the initial guess and the prescribed error limit . By this process the resistivity and depth values of each VES is quantitatively determined. From results of the sounding curve and the inversion, apparent resistivity pseudosection and geoelectric sections are constructed which indicate the electrical stratification of the studied area.

2.4 RESULT AND DISCUSSIONS

2.4.1 Geoelectrical sections

1. Profile1

According to the VES data along the first profile, the geoelectrical section has a four layered earth structure. The analysis of the geoelectric and pseudosections have provided useful information regarding the thickness and depths of layers Fig.(9).

he topmost layer is very thin with the range of thickness varying from 0.6m at VES 3 to 4.3 m at VES 2. The resistivity of this layer varies from 9 to 15 Ω .m. This result is signature of the alluvial cover.

The underlying low resistivity second layer is described by range of resistivity 3 to 9 Ω .m, and is representative of the clayey bed which extends to an average depth of 11 m from the surface.

The third geoelectrical layer is characterized by relatively wider resistivity that ranges from 12 Ω .m at the location of VES 1 to 210 Ω .m at VES 3. This is interpreted as weathered olivine basalt this considerable variations in resistivity may be due to variations in composition, degree of weathering or density of fractures. The low resistivity formation on this layer at the location of VES 1 seem to be continuation of the overlying clay bed intercalated with slightly coarse sand.

The fourth geoelectric layer is characterized by a relatively smaller value of resistivity (9-22 Ω .m). This small value of resistivity could be attributed to highly saturated volcanic ash and clay. The depth of the layer varies from 15m at VES1, to 195 m at VES 3.

By the method employed it was not possible to get high resistivity value which could be attributed to bed rock this is because the sedimentary material in the studied area is very thick so that even at $AB/2= 500$ m it was not possible to get bedrock response.

2. Profile -2 (VES 6 - VES 10)

The second profile is located at a distance of 500 m towards North of the first profile line. For this profile also geoelectric section was constructed and the result was analyzed Fig.(10).

The top layer is very thin with thickness ranging between 1-3 m the range of resistivity values observed varies from 12 -34 Ω .m. These values are attributed to a silty clay alluvial cover.

The second layer is described by low resistivity uniform layer with resistivity values below 7 Ω .m. The depth of this layer varies from 11 m at VES 9 to 30 m at VES 10. This layer is interpreted as clay.

The third geoelectrical layer is characterized by wider resistivity variations 66 to 115 Ω .m. This is interpreted to be weathered olvine and scoraceous basalt whereby the variation in resistivity could have resulted from differences in degree of weathering or composition and density of fracture. The thickness of this layer varies from 99 m at VES 10 to 160 m at VES 6. There is a possibility of ground water occurrence in this layer but the most favorable response is observed on the next layer.

The fourth layer is characterized by low resistivity value ranging from 20 to 50 Ω .m. This response comes from volcanic ash and mud.

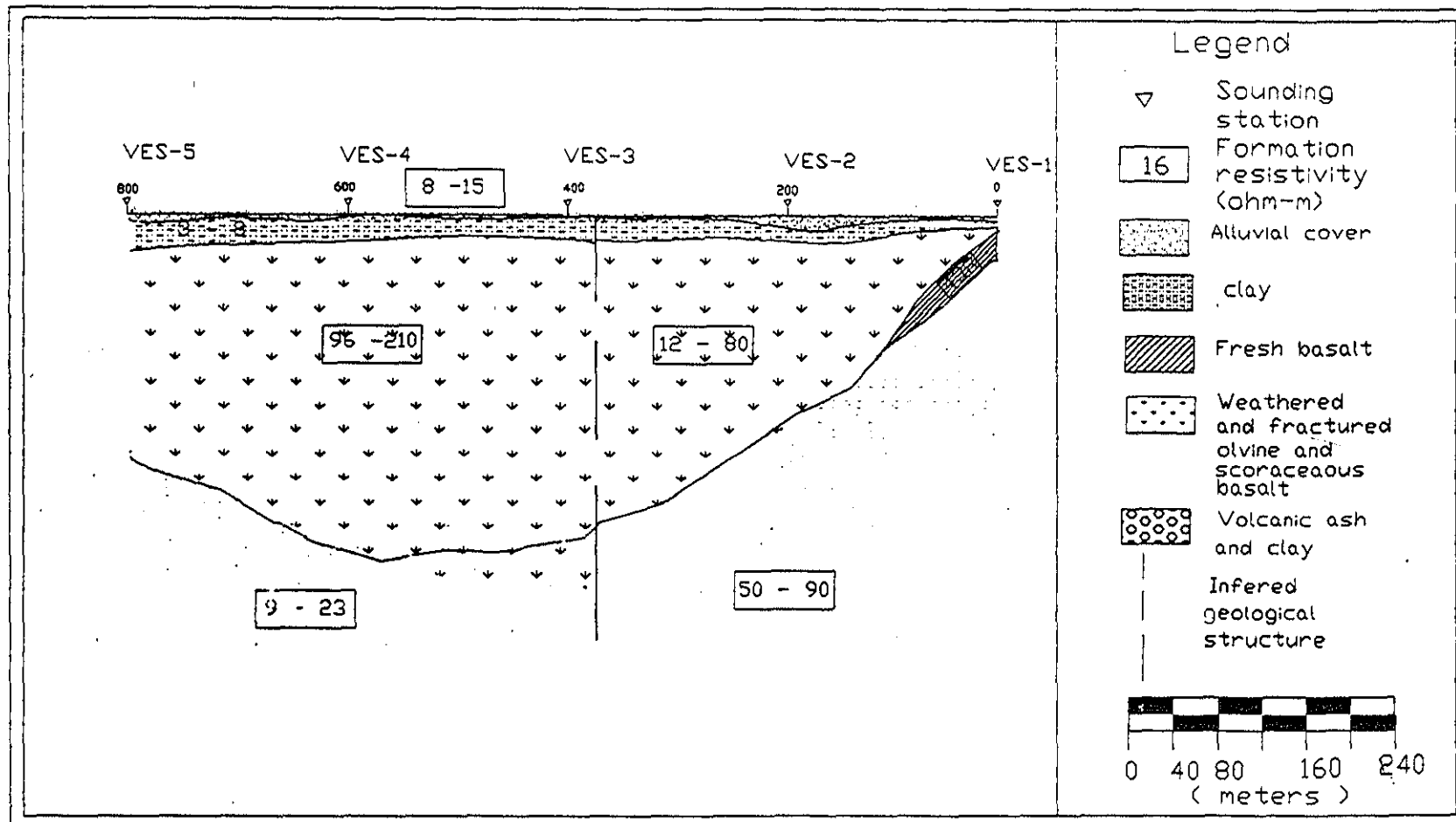


Fig. 7 Geoelectric section along profile 1

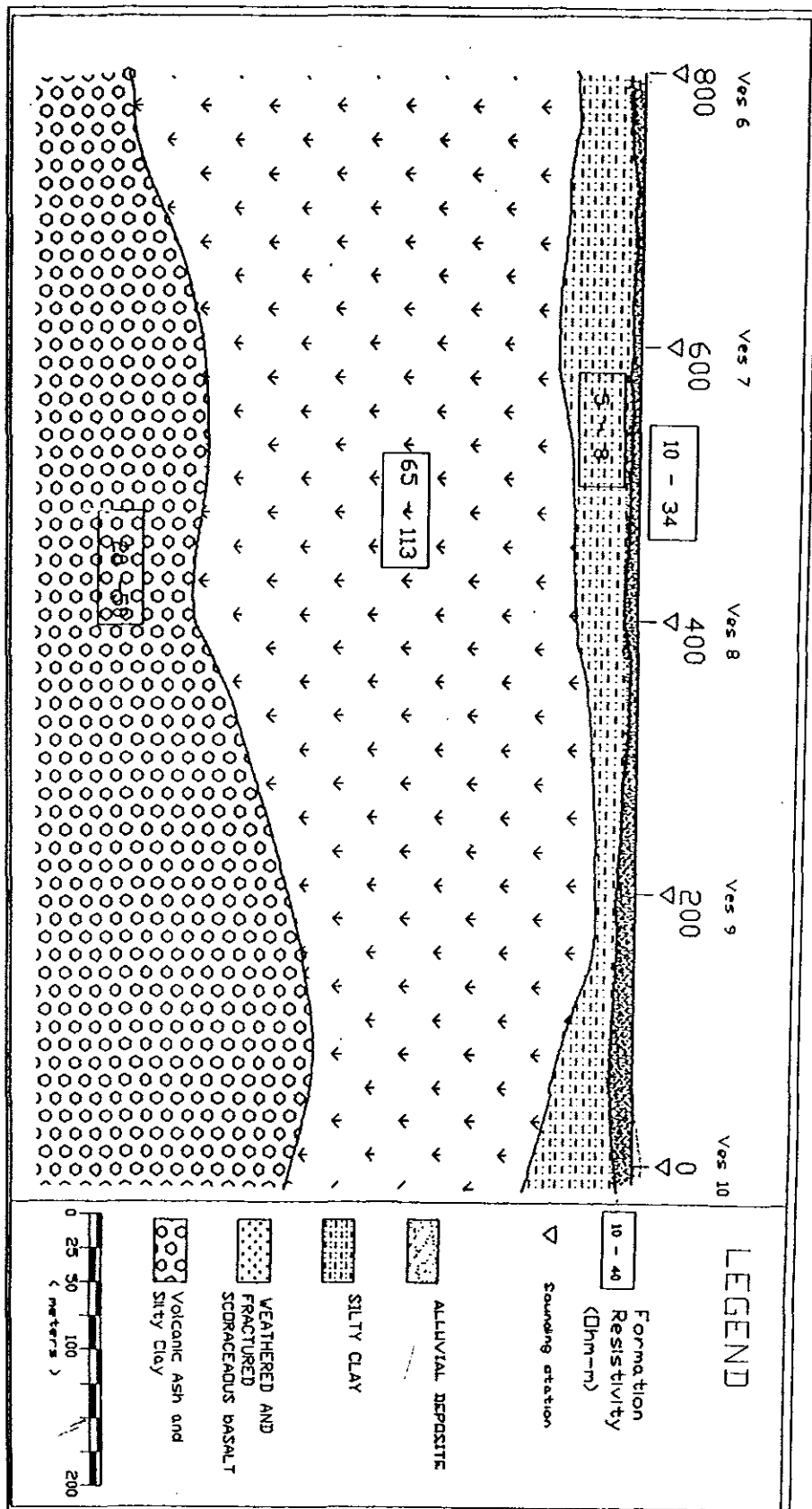


Fig.10 Geoelectric Section Along Profile 2, Dembi area.

3. Profile 3

The third profile line also 500 m towards north from the second profile and includes VES 11, VES 12, VES 13, VES 14 and VES 15. Likewise the previous profile the electrical section of this profile Fig(11) describes a first layer of very thin alluvial cover of silty clay composition with resistivity ranging 8-36 $\Omega.m$ and thickness varying from 0.9m to 4m. This layer reaches its maximum thickness 4m at the location of VES 14.

The underlying second layer is characterized by small resistivity value 3-12 $\Omega.m$ which could be interpreted as the response of clayey bed. This layer is also defined by a more or less uniform thickness along the profile and the average depth to this second bed is 22 m.

The third geoelectric layer of this profile is described by resistivity values ranging from 10 - 55 $\Omega.m$. This layer is characterized by a highly weathered and saturated basalt. The thickness of this layer reaches its maximum at the location of VES14 where it is about 145 m whereas at VES 13 it is shallower. This layer is also highly saturated and hence could be hydrogeologically important. The underlying fourth layer has resistivity value lying between 30 to 40 $\Omega.m$ and this is the response of volcanic ash and silty clay intercalated with coarse sand. This fourth geoelectric section is shallow at VES 13.

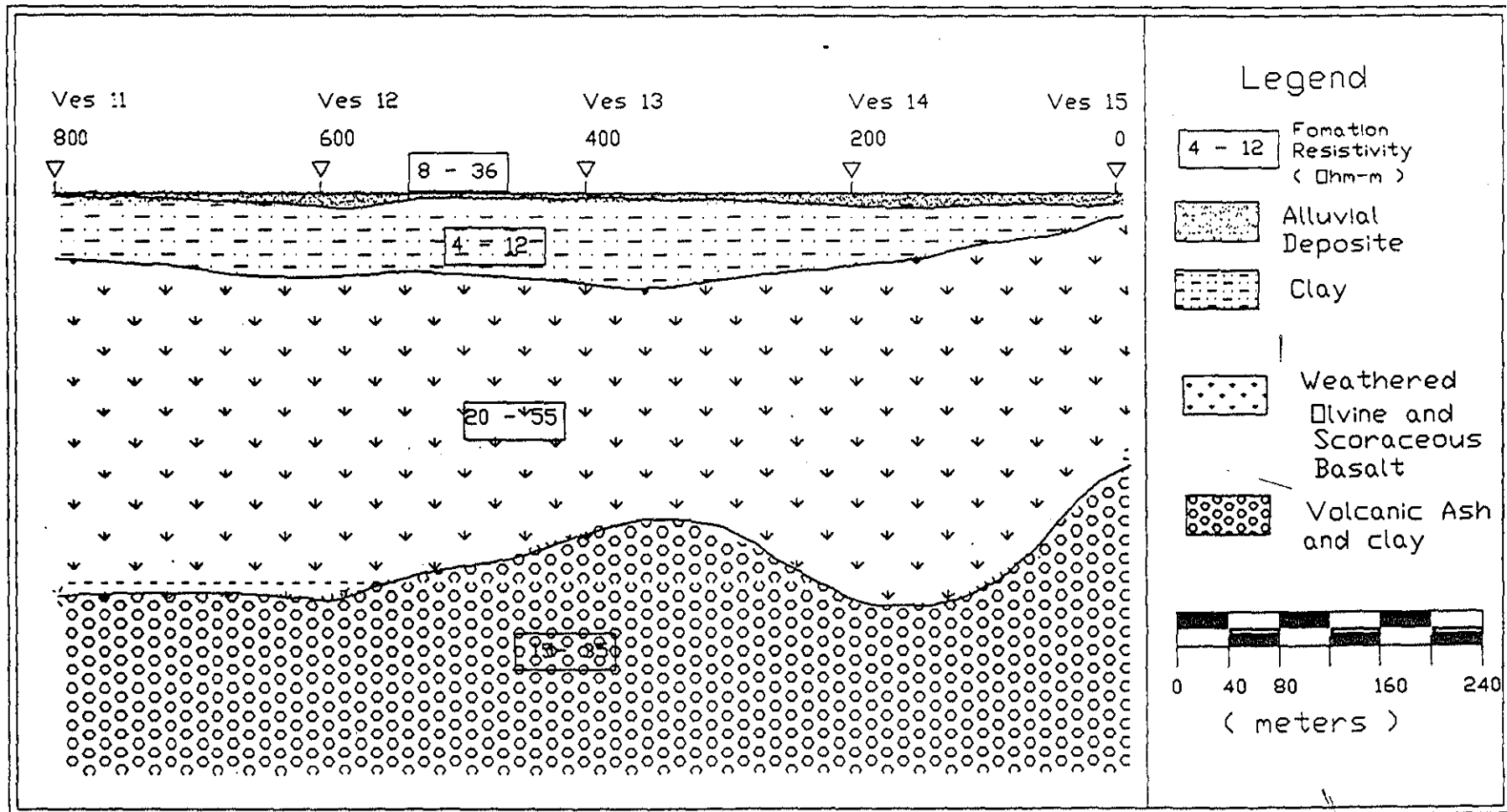


Fig.// Geoelectric section along profile 3

about the bedrock in which our study failed to map even at AB/2 500 because of the high thickness of the sedimentary section.

4. Profile 4

This profile is also 500 m from the above discussed profile line on the further side of the studied area towards Yerer mountain. This area is characterized by comparatively lower resistivity ranging from 5 to 60 Ω .m for all of the four layers Fig.(13) and hence could be zone of infiltration for the surface runoff which comes from the mountainous area in the northern side. This could be discerned not only from the geoelectrical point of view, but also from the well developed drainage pattern it is justifiable. As in the previous cases the first layer is very thin, varying in thickness from 0.5m at VES 20 to 2.5m at VES 19. The resistivity response obtained suggests that it is alluvial cover of black clay soil with range of resistivities for this layer between 10 to 12 Ω .m

The underlying bed is of low resistivity value ranging from 5 to 7 Ω .m which could be interpreted as a fine clay bed. The depth to this layer is shallower at the location of VES 17 which is 18 m where as it is thicker at VES 20 which is about 37 m.

The third layer is characterized by resistivity range from 20 - 40 Ω m which could be attributed to a highly weathered and fractured basalt. This layer exhibits highly undulating structure across the profile showing shallower depth at VES 17 and abruptly deepens to a depth of 220 m at VES 18. This layer like the case of the

third profile, shows low value that could be response of volcanic ash and clay. The resistivity of the fourth layer ranges from 16 - 60 Ωm .

From the resistivity responses of the third layer it is possible to suggest that it could be the possible aquifer but since the characteristics of the bed rock is not confirmed by the method employed, hence, it may not be possible to surely suggest that it is an important ground water reservoir.

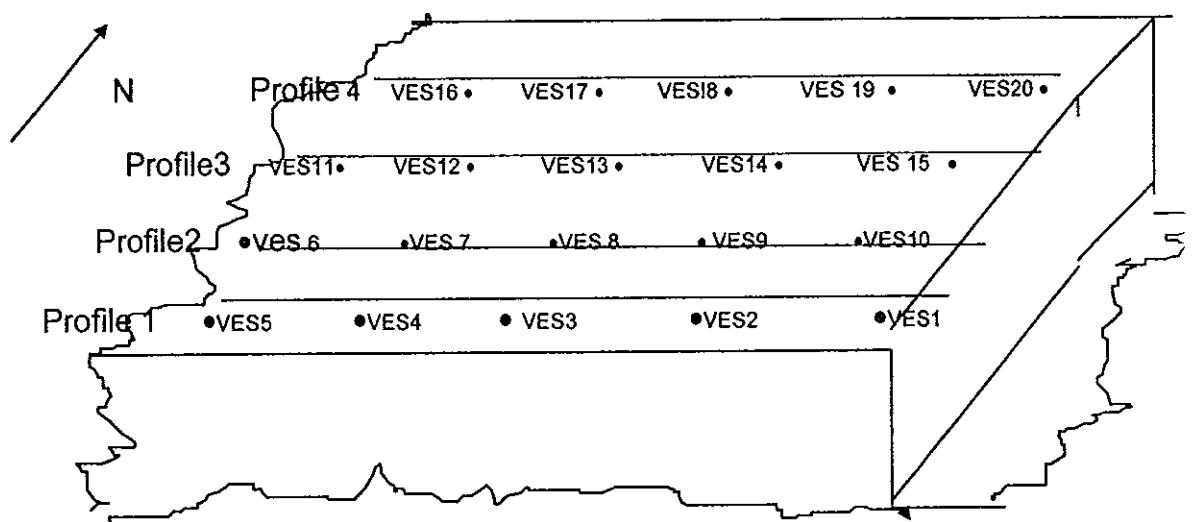
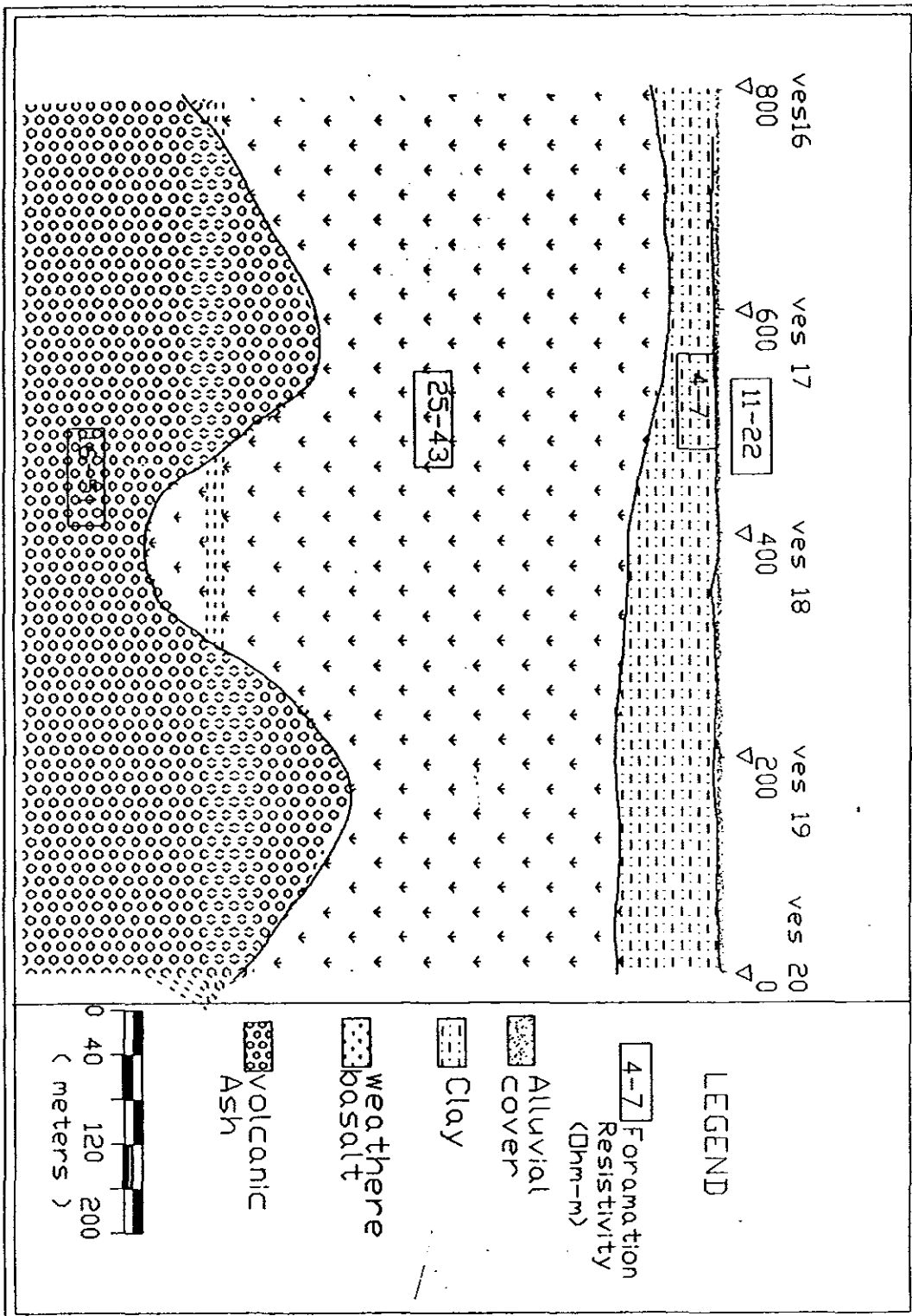


Fig.(12) schematic diagram showing sounding stations and profiles

Fig. 5. Geoelectric section along profile 4, Direbotte area



2.4.2 Pseudosection

The apparent resistivity values are also presented in the form of pseudosection which qualitatively shows the lateral and vertical variations of electrical properties with in the subsurface.

Profile 1

Based on the apparent resistivity pseudosection corresponding to the first profile Fig.(14), it is observable that the near surface zone is characterized by apparent resistivity values in the range of 15 - 35 Ωm . There is no clear indication of lateral discontinuity and hence near surface layers show uniform electrical behavior across the profile. But it is observable that changes in resistivity are significant with depth. At shallower depth at the location of VES1 it is observable that there is relatively higher resistivity. The middle part of the pseudosection is characterized by higher resistivity (45-90 Ωm) with a general decreasing trend towards the western profile (VES 6) (10 - 35 Ωm) apparent resistivity values of 20-45 Ωm is observed at very great depths.

Profile 2

From apparent resistivity pseudosection of the second profile Fig.(15) the near surface zone is characterized by apparent resistivity values in the range 10-25 Ωm with no lateral discontinuity of the layers. But the extreme top right and left margins show relatively high resistivity value. The middle zone is characterized by intermediate resistivity values in the range 20-40 Ωm and is also horizontally undisturbed except that it deepens at the two extreme ends of the profile reaching

maximum depth at the location of VES6. The bottom part of the pseudosection shows higher resistivity values 40-55 Ωm where the maximum resistivity is shown as a localized portion beneath VES9 .

APPARENT RESISTIVITY PSEUDOSECTION PROFILE 1

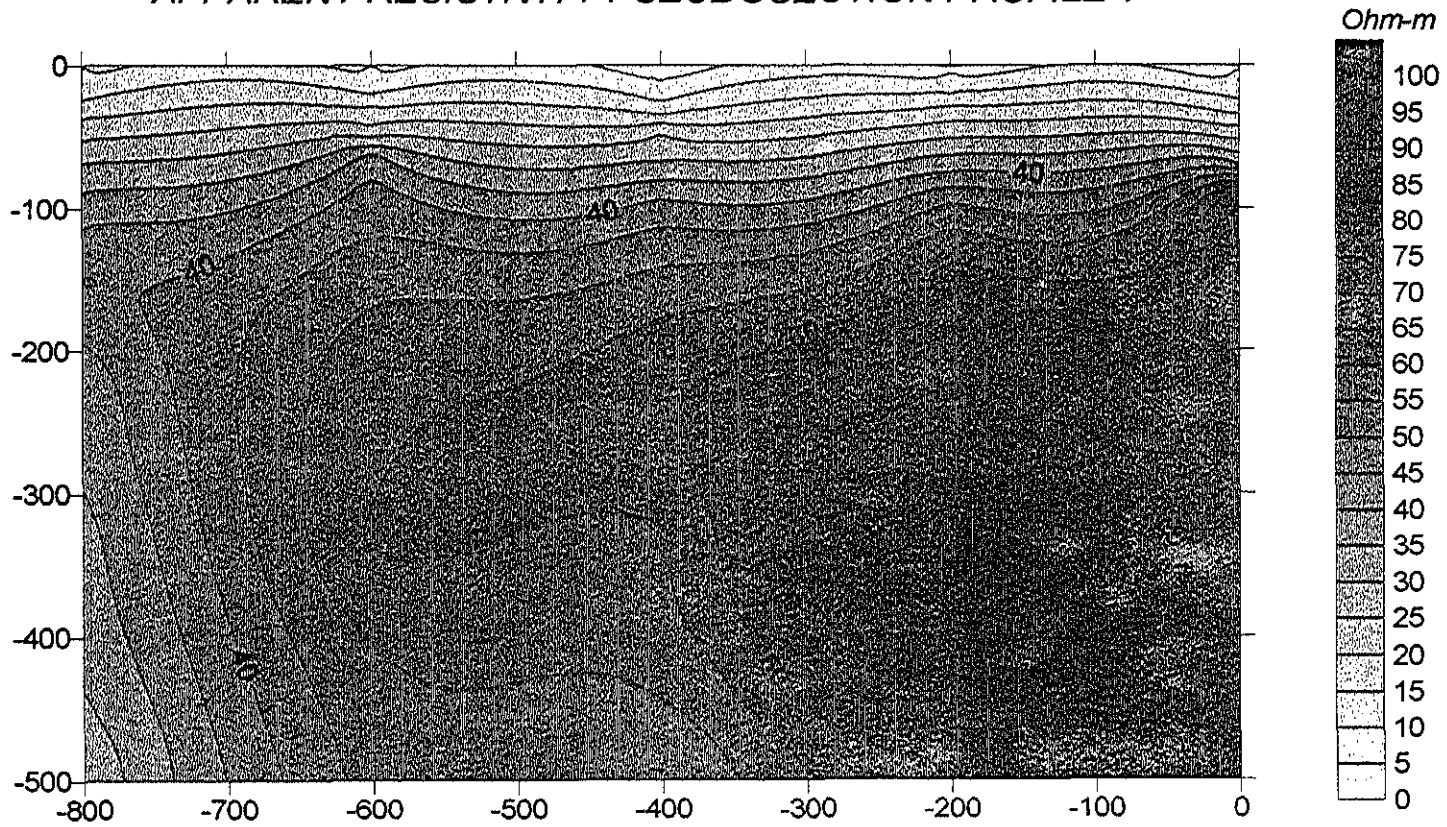


Fig 14

APPARENT RESISTIVITY PSEUDOSECTION PROFILE 2

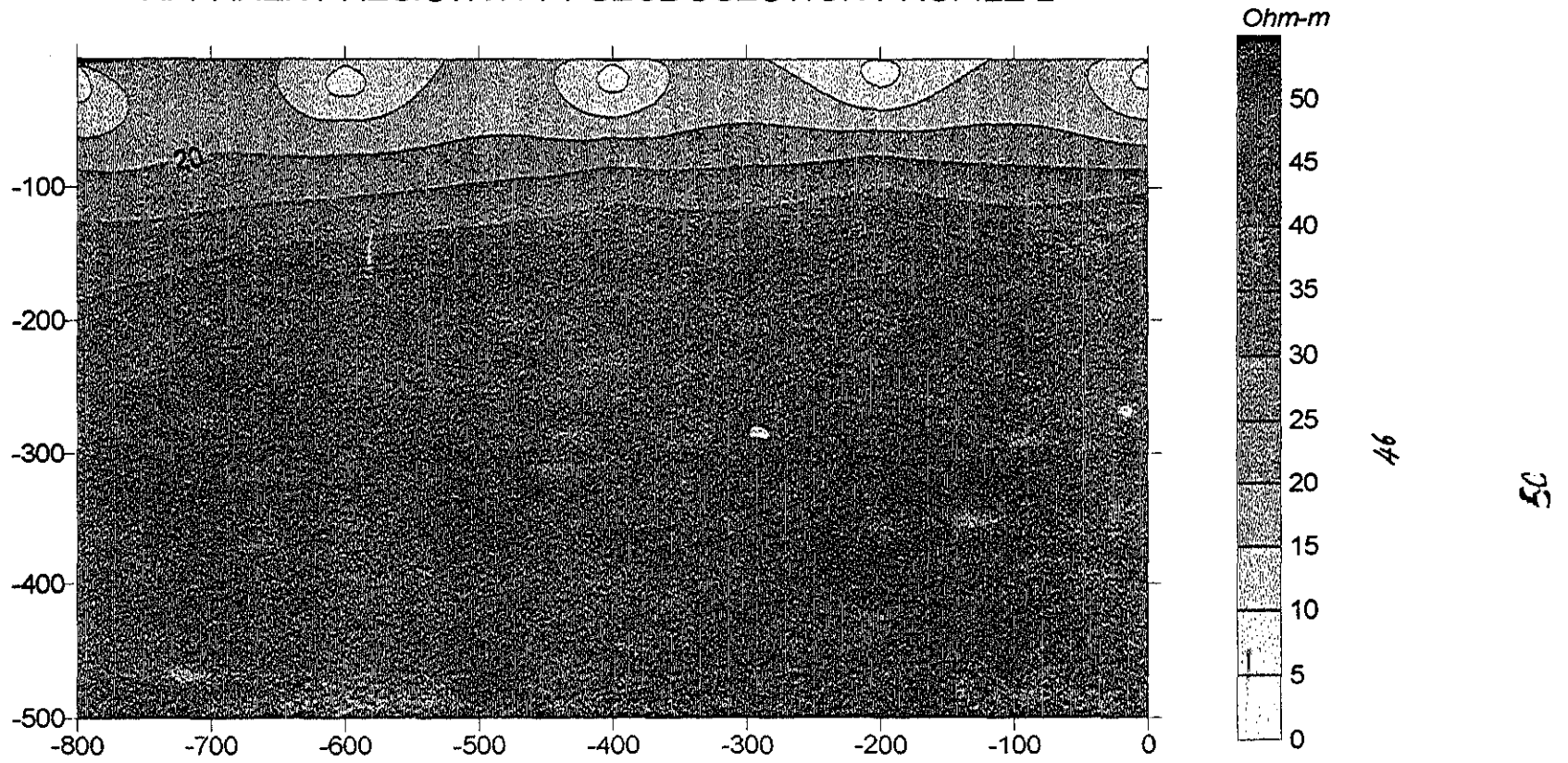


Fig 15

Profile 3

This profile is located near a settlement called Yatu. The overall resistivity range for this profile is small (5-35 Ωm) Fig.(16) as compared to the previous profiles. From the apparent resistivity pseudosection it is observable that there is lateral inhomogeneity of the upper layer. High apparent resistivity values are observed on the eastern side of profile with a decreasing trend towards west (VES 11). From the low resistivity value of the subsequent layers, and the lateral inhomogeneity of the top layer, especially the top left portion of the pseudosection could suggest a zone which may serve as a conduit for segregation of water to the possible aquifer at the bottom. The middle zone is characterized by low apparent resistivity values (5 -15 Ωm) this zone is found at shallower depth at the location of VES 15 to VES 13, whereas it attains its maximum depth at VES 12. At greater depth the apparent resistivity shows higher values > 25 Ωm .

Profile 4

This is the last profile located 500 m from the third profile near a small settlement called Direbotte. By lateral view of the apparent resistivity pseudosection corresponding to this area Fig(17), it is possible to discern continuous resistivity distribution of the upper layer except at the position of VES 19 and VES 18 which shows comparatively high values than the neighboring stations.

The middle layer is represented by apparent resistivity values 15-20 Ωm , the contour pattern is very similar to that of the third profile in that it deepens towards the western profile reaching maximum depth at VES17 which is exactly parallel

station with VES12 of the third profile. The contour pattern is an indicator of similar geologic setting which traverses perpendicular to both profiles. The bottom most layer is described by high resistivity values and depth to this layer increases towards VES16.

APPARENT RESISTIVITY PSEUDOSECTION PROFILE 3

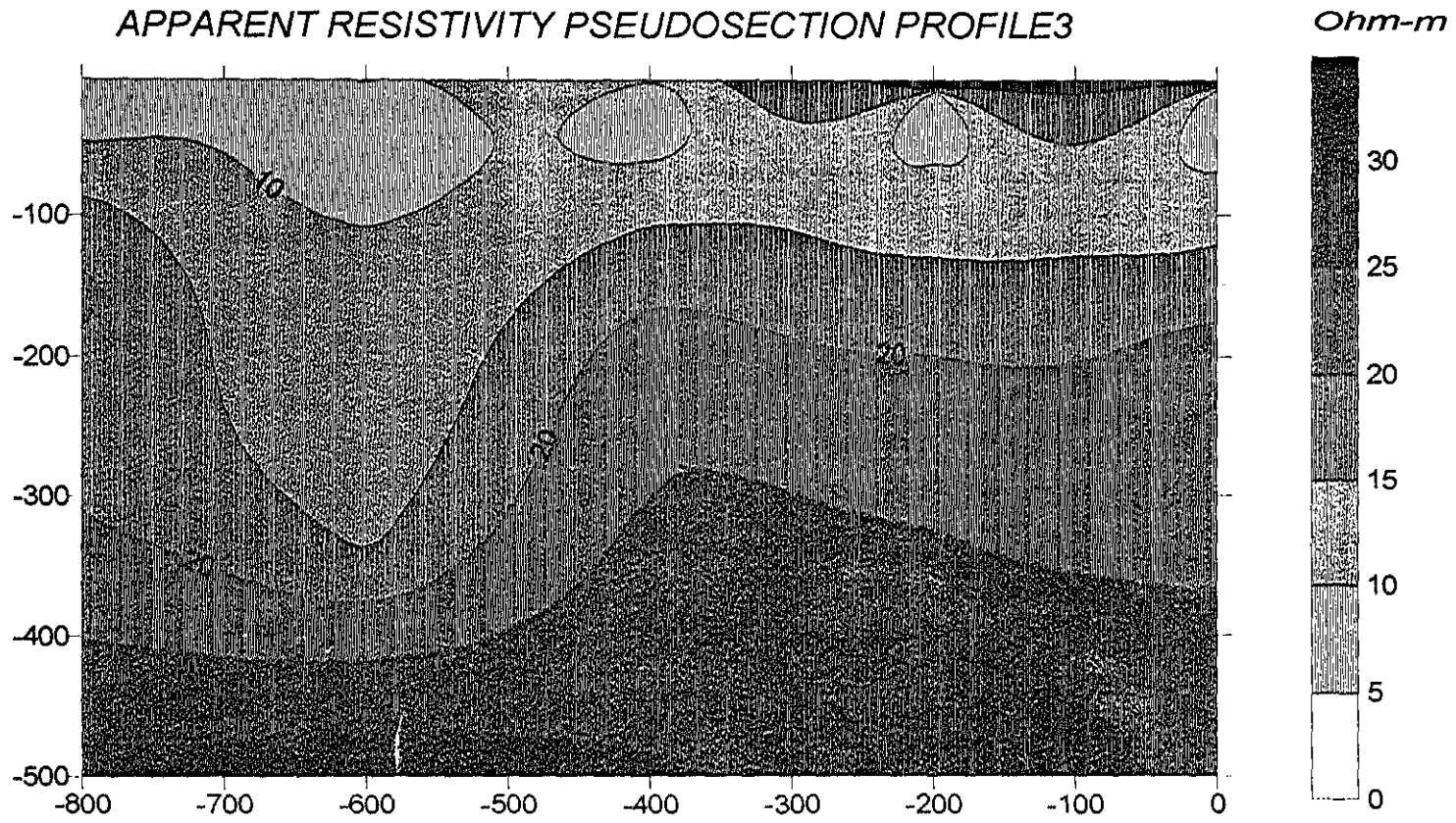


Fig 16

2.4.3 Apparent resistivity contour

From a traverse of sounding stations, section of apparent resistivity space can be constructed where sounding stations are plotted horizontally and the apparent resistivity values are assigned below each station location at a "depth" equal to half the spacing used. Such an observed space section can be summarized by contours of apparent resistivity. This kind of representation is very important in that it gives a visual picture of the whole area which is investigated. The procedure enables the results to be interpreted in terms of overall geological setting rather than individual locations. Furthermore, this technique maybe of great use qualitatively in siting regions where intensive investigation is required or it is believed to reveal the observed field results in a convenient form that it is able to show the apparent resistivity distribution for the whole area of study in terms of electrode spacing and position (Z.M.Zafran,1981)

Therefore, apparent resistivity contour maps for different values of $AB/2$ are mapped to see the lateral distributions of electrical behavior of the layers which may be of great interest for siting drilling points.

If one considers the apparent resistivity contour map constructed for $AB/2=45$ Fig.(18), it is possible to observe high values (28 ohm.m) for the first two profiles with decreasing trend towards the fourth profile attaining a value of very low resistivity of $8 \Omega m$.

If we observe the apparent resistivity distribution for the contour map constructed for $AB/2=100$ Fig(19), it clearly shows high values at the location of VES1 of the first profile and shows that the bedrock is nearer towards the first profile whereas

towards the fourth profile very small values are displayed. The apparent resistivity values observed at $AB/2=100$ show a decreasing trend from VES1 to VES5 of the first profile. But the value which is observed is very small as one goes perpendicular to the profile lines attaining the smallest at the location of profile 4. Even at $AB/2=150$ Fig.(20), the contour map shows a decreasing trend from the first to the fourth profile but there is no significant variation along the profile line. Changes are rather significant across(perpendicular to) the profile lines.

When one observes the apparent resistivity contour map constructed for $AB/2=220$ Fig (21), bed rock responses are seen at the location of the first profile line whereas the value of apparent resistivity is still small(12-20 Ωm) at profiles 3 and 4.

For the case of contour maps constructed for $AB/2=500$ Fig.(22), it is possible to observe the apparent resistivity changing both along the profile and across the profile with lateral changes from 56 to 28 Ωm .

APPARENT RESISTIVITY CONTOUR MAP FOR $AB/2 = 100$

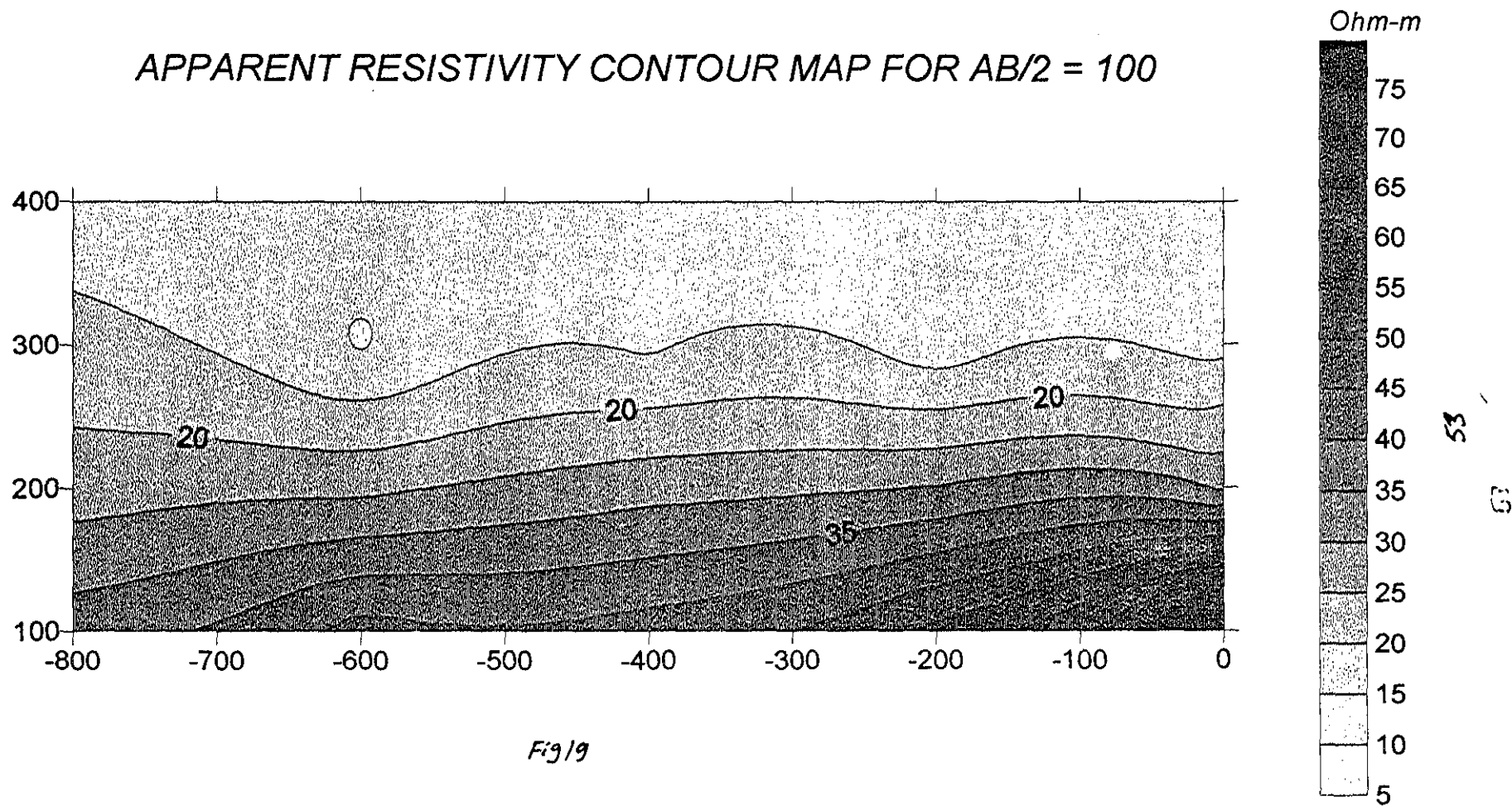


Fig 19

APPARENT RESISTIVITY CONTOUR MAP FOR $AB/2 = 150$

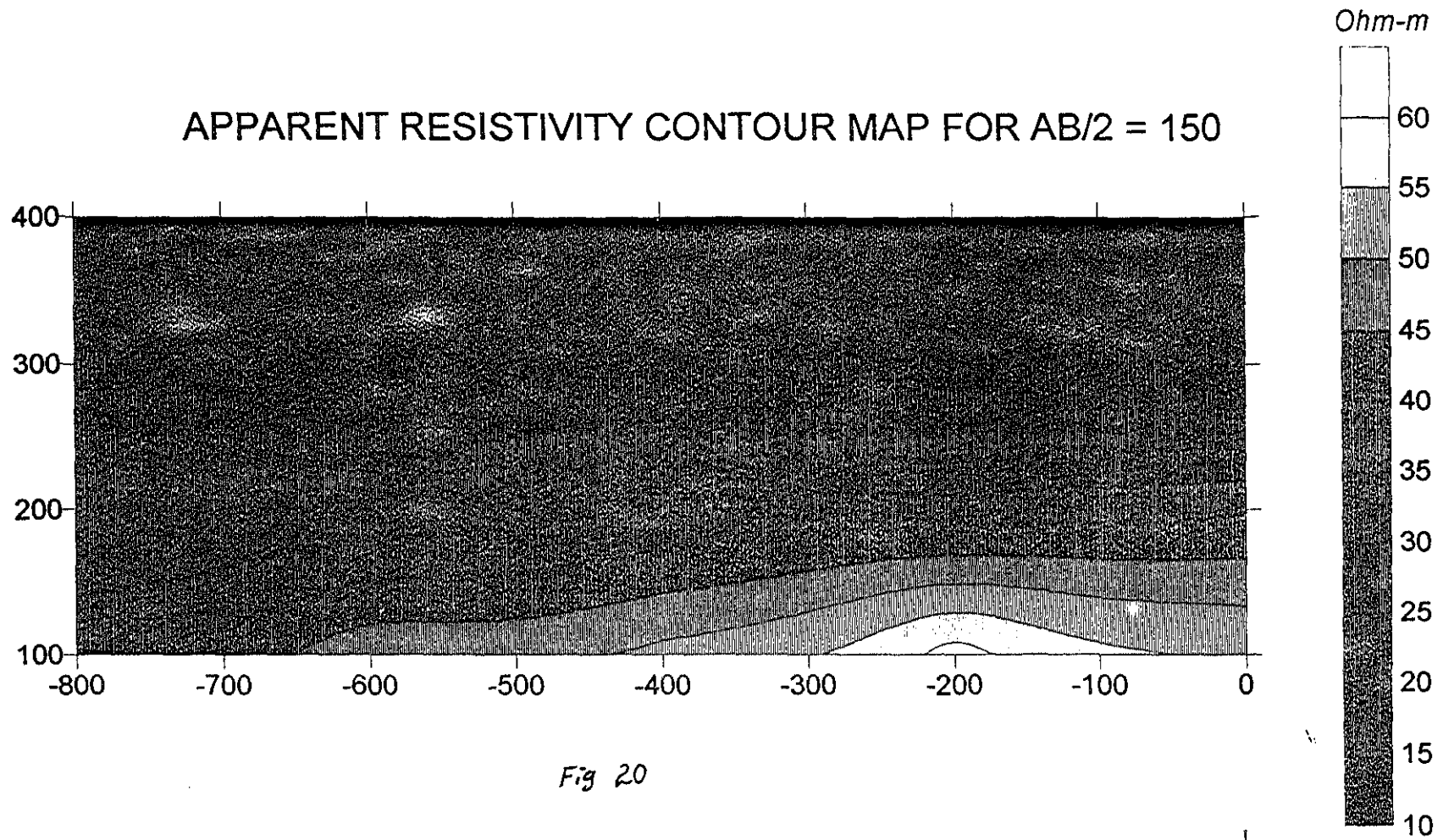


Fig 20

APPARENT RESISTIVITY CONTOUR MAP FOR $AB/2 = 220$

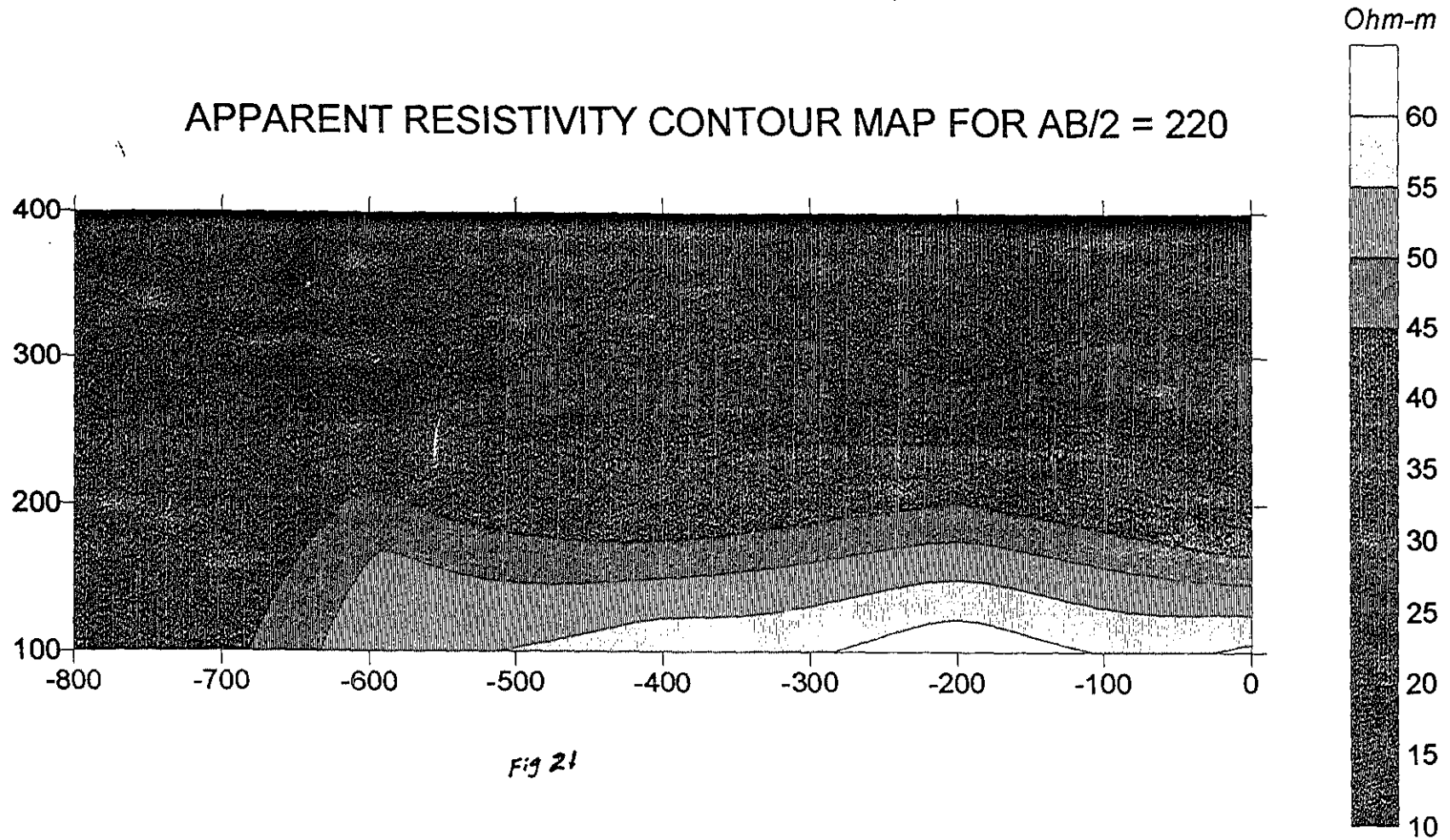
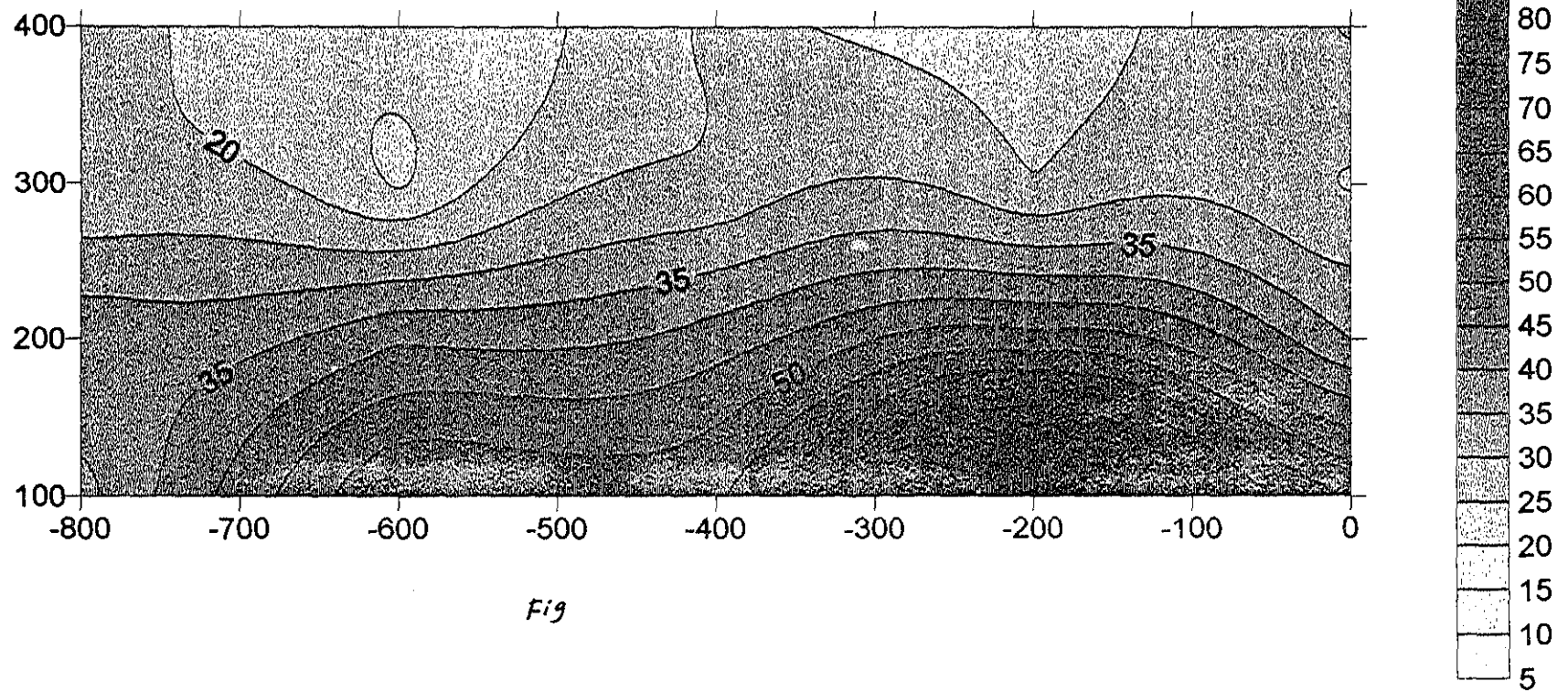


Fig 21

APPARENT RESISTIVITY CONTOUR MAP FOR $AB/2 = 330$



Fig

APPARENT RESISTIVITY CONTOUR MAP FOR $AB/2 = 500$

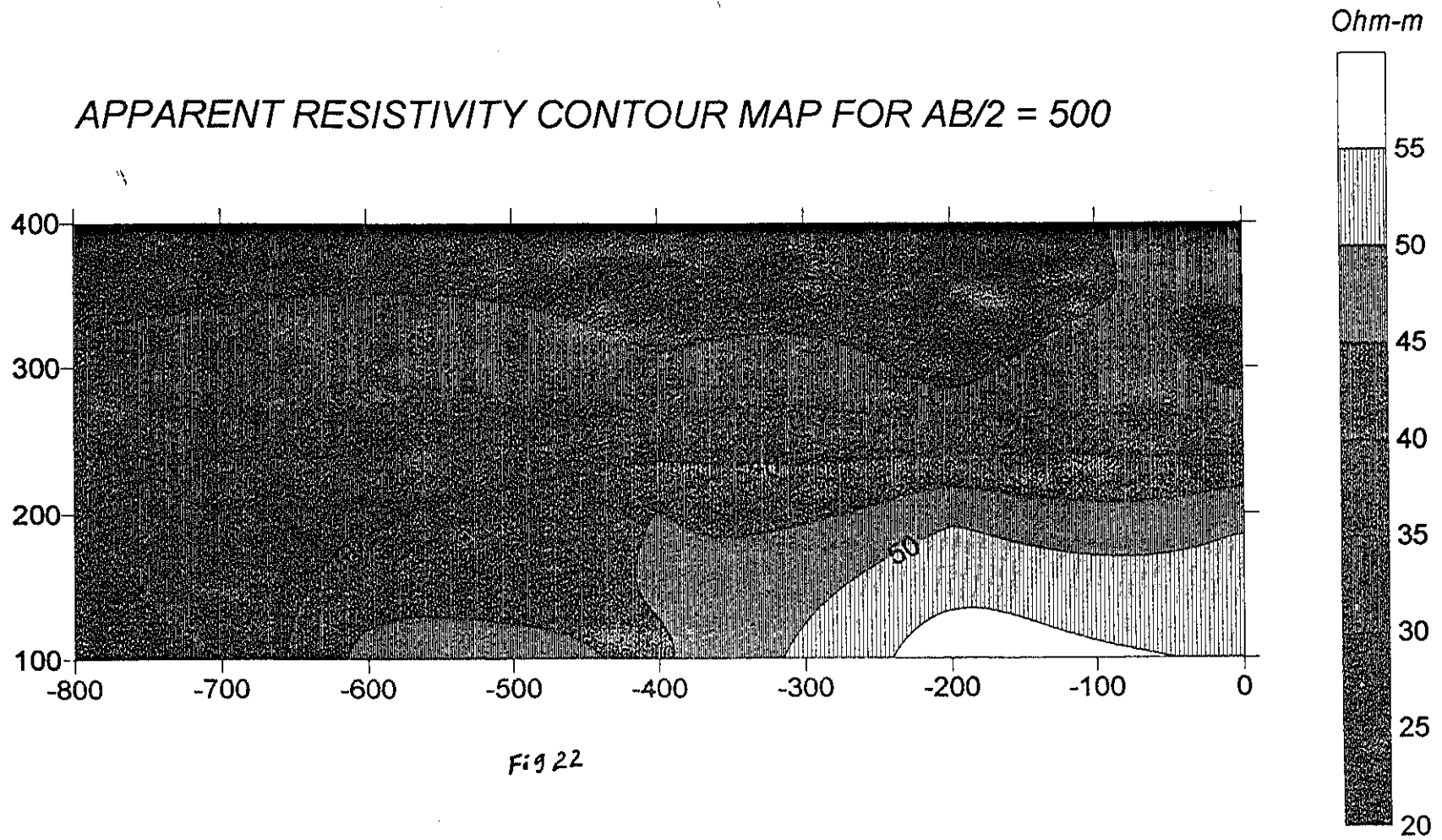


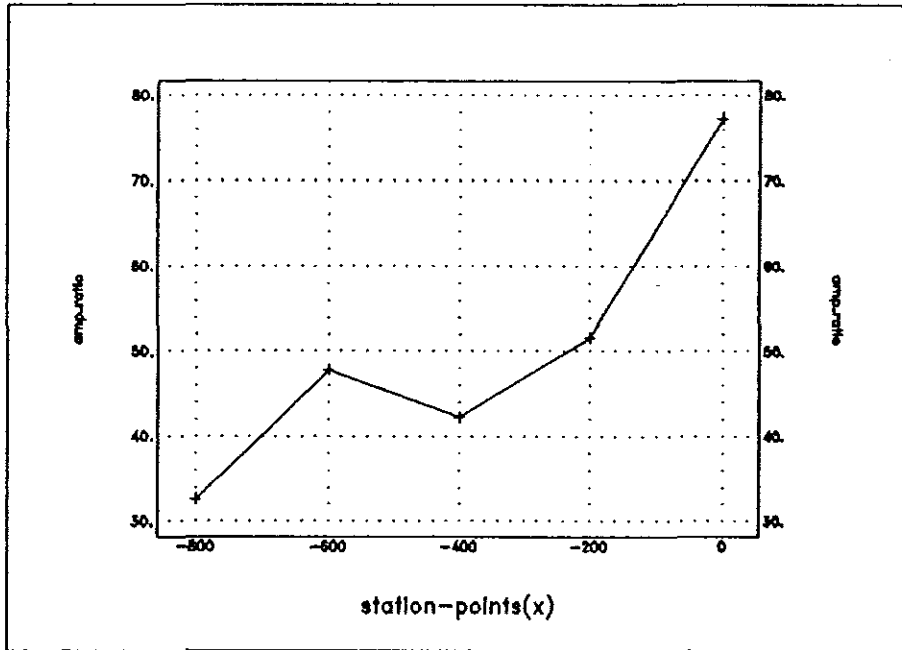
Fig 22

VES 5 at this specified depth. This agrees with the results obtained for the third geoelectric layer by the sounding interpretation and such variation in the observed apparent resistivity value could be attributed to the changes of the relatively fresh olivine basalt response of VES 1 which is observed to change to highly weathered bed rock response of the western profile.

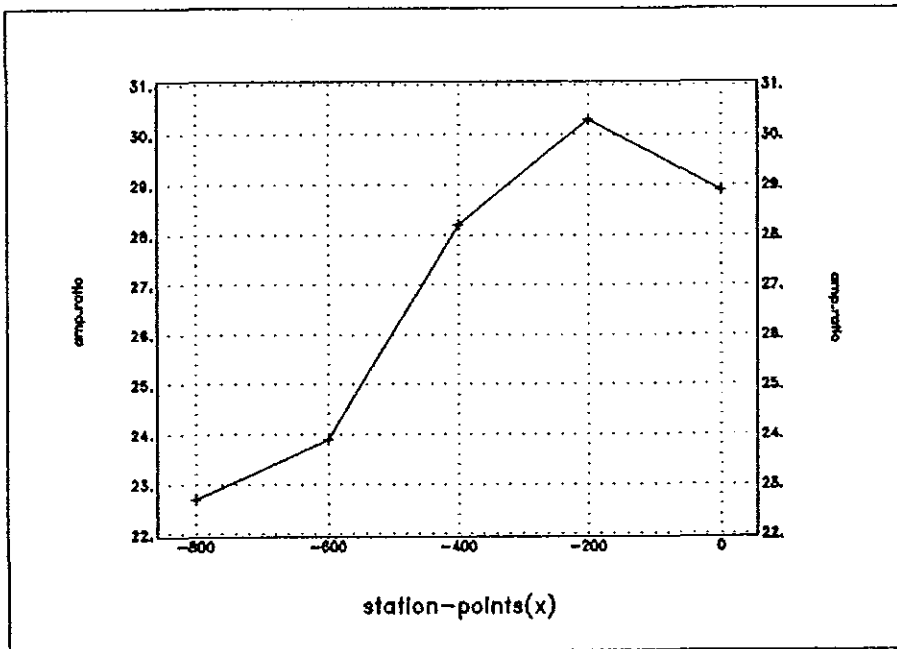
Profile plot of the second profile for the same $AB/2=100$ (23b) also shows a general decreasing trend towards the western profile. Both the magnitude and the range of resistivity variations are very small as compared to the results obtained for the first profile, at the same depth. The changes observed at this specified horizon is due to variations in the degree of weathering of the sandy bed which is esteemed to be the probable aquifer. But, some resistive body is observed at 200W(VES 9) of the profile.

Analysis of the results of the third profile plot at the same depth level Fig.(23c) shows an increasing resistivity towards the west except at the VES 12 which shows a sharp decrement which is response of conductive body. The overall result describes the horizon is very conductive as compared to the first two profiles discussed for similar depths.

Consideration of the plot corresponding to the fourth profile for the same AB shows more or less uniformly conductive horizon except at the location of VES 20 which shows a comparatively high value Fig.(23d).

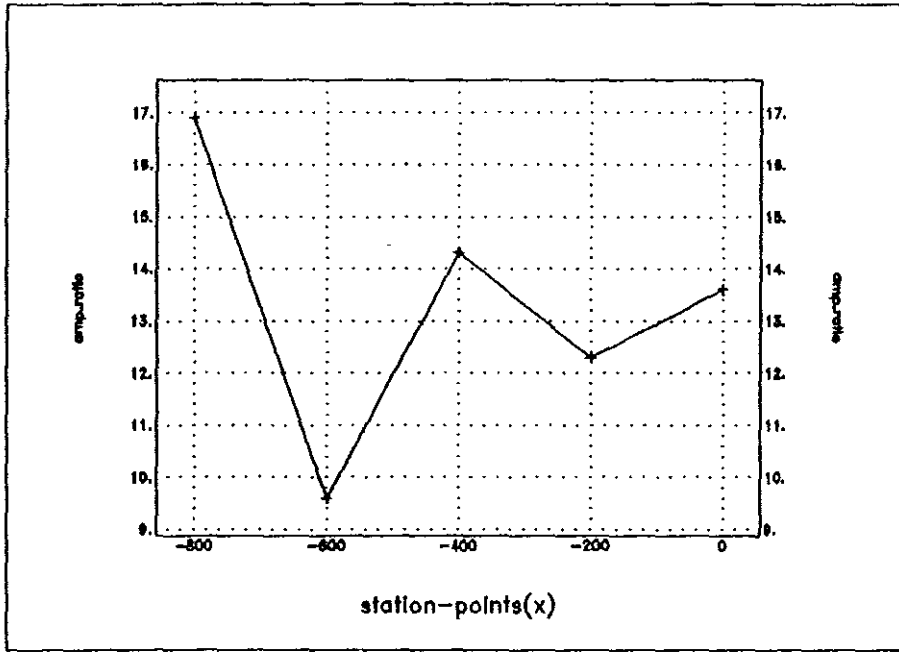


23a

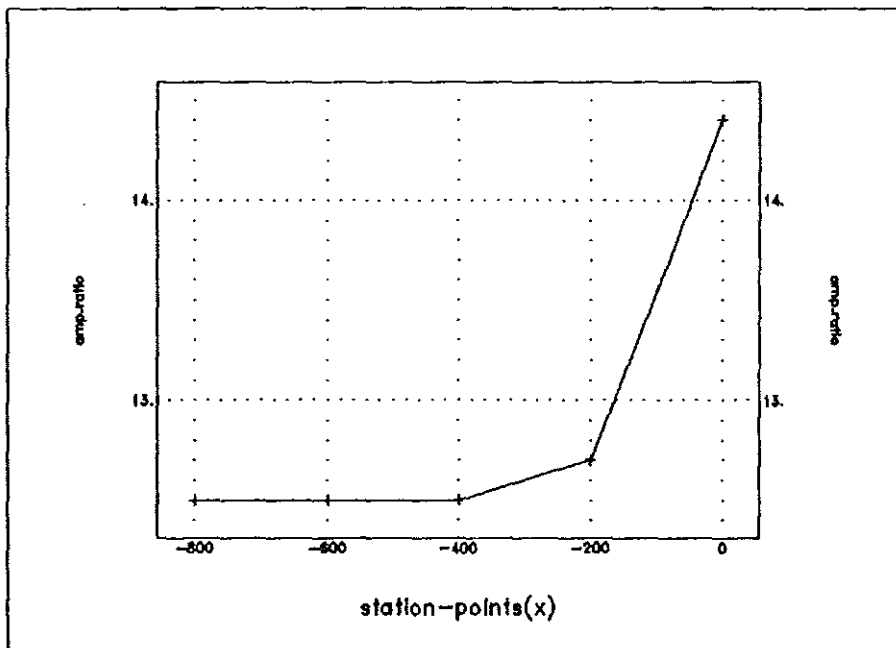


23b

Fig.(23a),(23b)Profile plot for the first and the second profiles for $AB/2=100$



23 c

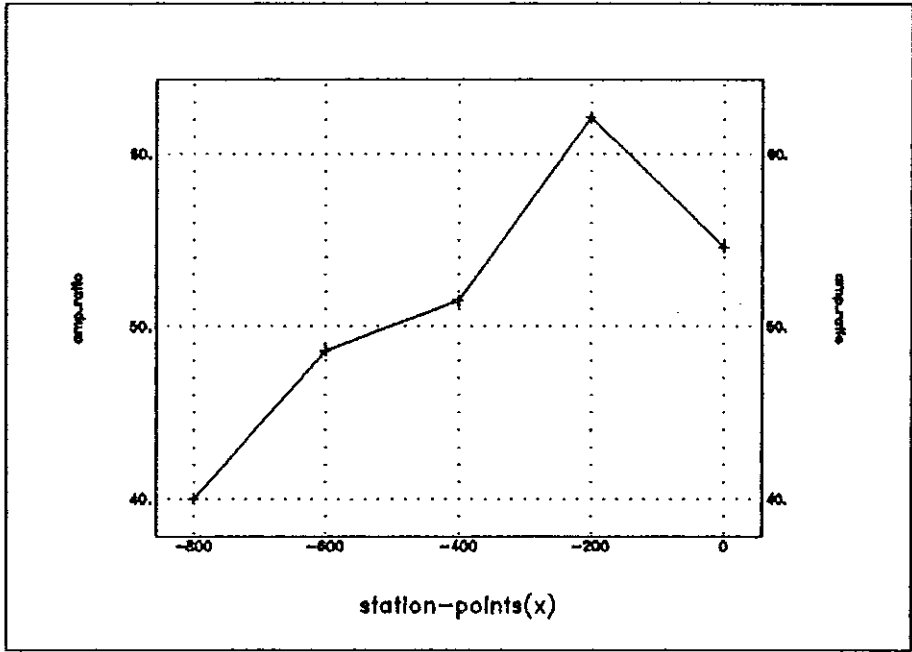


23 d

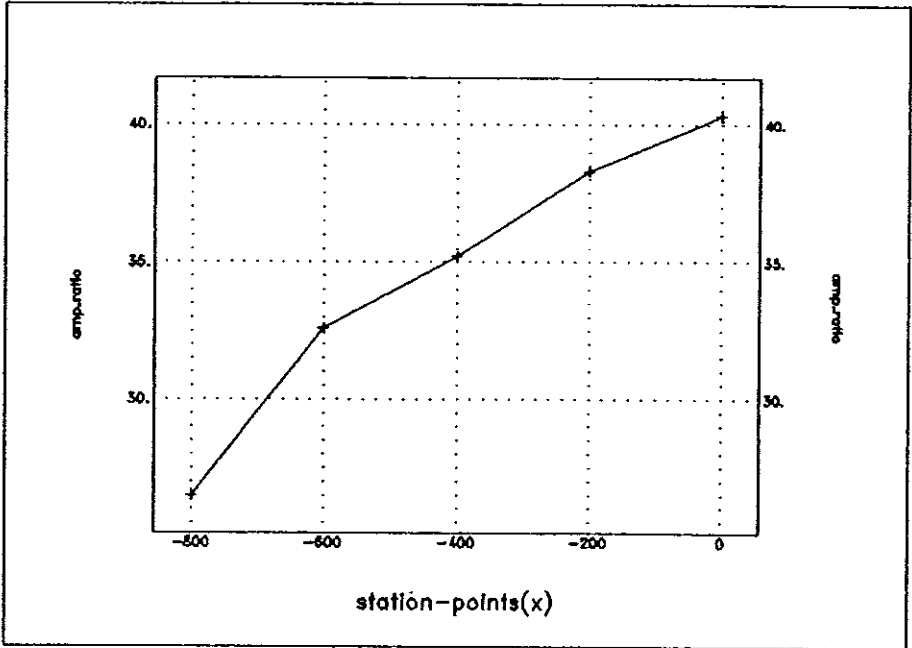
Fig.(23c),(23d)Profile plots for the third and fourth profiles for $AB/2=100$

Studying the plot obtained for $AB/2=150$ for the first profile there is a decreasing apparent resistivity value to the western profile for this depth level also some resistive body is observed exactly at parallel station at 200 W(VES2) Fig(24a). The results depict weathered bed rock responses where by variations on apparent resistivity value from 64 to 40 ohm. m might be consequences of weathering and fracturing of the zone. The results of the second profile plotted for similar $AB/2=150$, Fig.(24b) shows a decreasing trend on apparent resistivity towards the west like the previous cases, but, the decrement is some what gentle as compared to the other profile plots. The corresponding picture for the third profile for $AB/2=150$ Fig(24c) unlike the other cases shows an increasing resistivity trend except at the location of 600 W, which showed very low value like what is observed for the same station at $AB/2=100$. The corresponding fourth profile plotted for the same $AB/2$ Fig.(24d) showed the usual tendency of decreasing towards the west.

Profile plot is also generated for depth corresponding to $AB/2 = 330$ m for all profiles in the survey area and results were analyzed. The result shows some anomalously resistive body at 200 W on both the first and the second profiles (i.e. at VES2 and VES9) which describes the existence of some geologic body which goes perpendicular to both profiles crossing exactly similar stations on the two parallel profiles Fig(25a)and Fig(25b). This body started to appear at the same station at $AB/2=100$ at profile 2, at $AB/2=150$ at profile 1 and still observed at $AB/2=330$ analysis of the observed body suggests that it is a dyke like geologic body which is traversing perpendicular to the two profiles. The width of this body extends from 0 to 400W. Consideration of the third



24a



24b

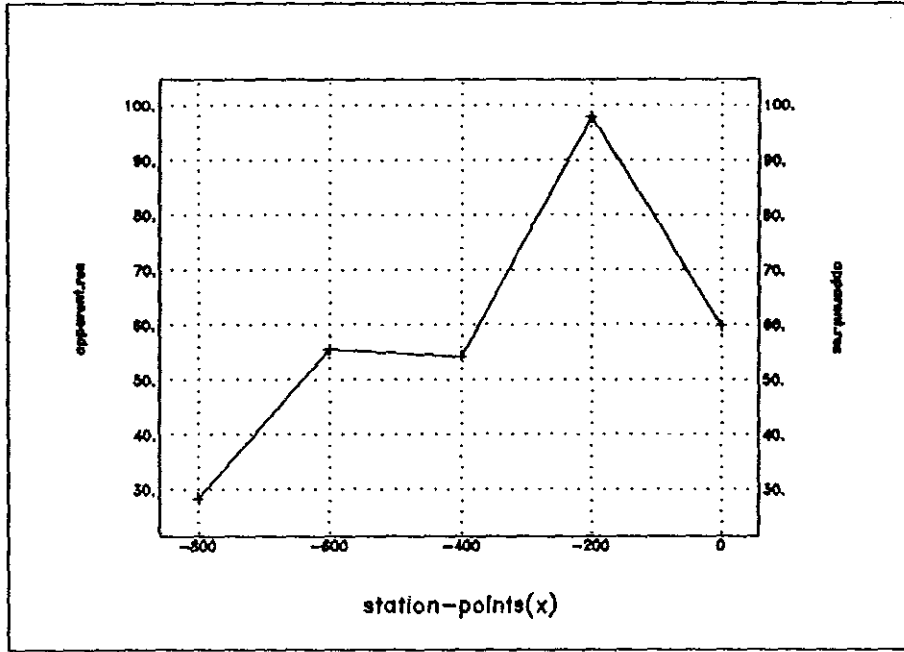
Fig.(24a) and fig.(24b)

and the fourth profile plots shows an over all decreased magnitude of apparent resistivity which might be consequences of saline water bearing conductive zone Fig(25c) and Fig.(25d). There is also anomalously conductive zone which is observed crossing Both parallel profiles at VES 12 and at VES 17 which are exactly parallel stations perpendicularly (It has been seen at 600W starting from $AB/2=100$). This could either be explained by the high degree of weathering of the scoraceous basalt or maybe associated with the degree of dissolved salt concentration that might be high.

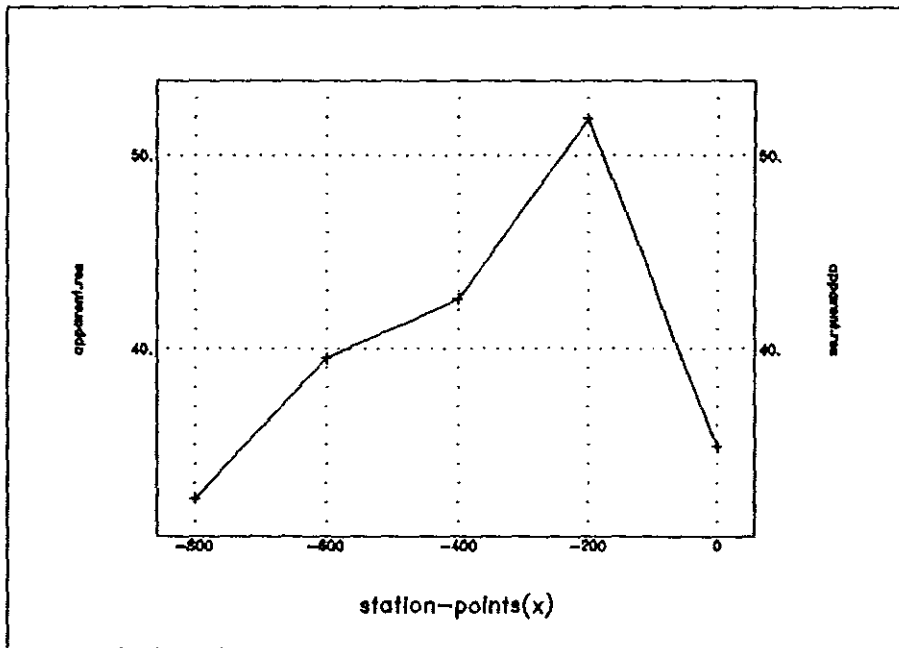
Profile plot which is constructed for $AB/2=500$ is also analyzed and the result depicts that the bed rock response observed for the first profile shows a gently decreasing trend towards the western profile Fig(26a). The magnitude of the response to wards the extreme west is so small that it may not be bed rock response. The result of the second profile plot constructed for the same $AB/2 = 500$ is similar to the first profile and hence analogous explanations may be equally valid for this case Fig.(26b).

The result of the third profile plotted for $AB/2=500$ shows generally small apparent resistivity values describing the conductive nature of the area. What is observed in this horizon which is not seen in the other discussions above is an unusual increasing trend of electrical response towards the west Fig(26c). In all the previous discussions the response obtained beneath 600 W (VES.12) of the third profile was being described by anomalously conductive for cases considered for different depth corresponding to $AB/2=100, 150,330$ but when we come to the depth corresponding to $AB/2=500$ the same place is identified by comparatively higher values of apparent resistivity. When we consider the fourth profile plot

generated for the same depth level ($AB/2=500$) the usual west ward decrement is again observable Fig.(26d).

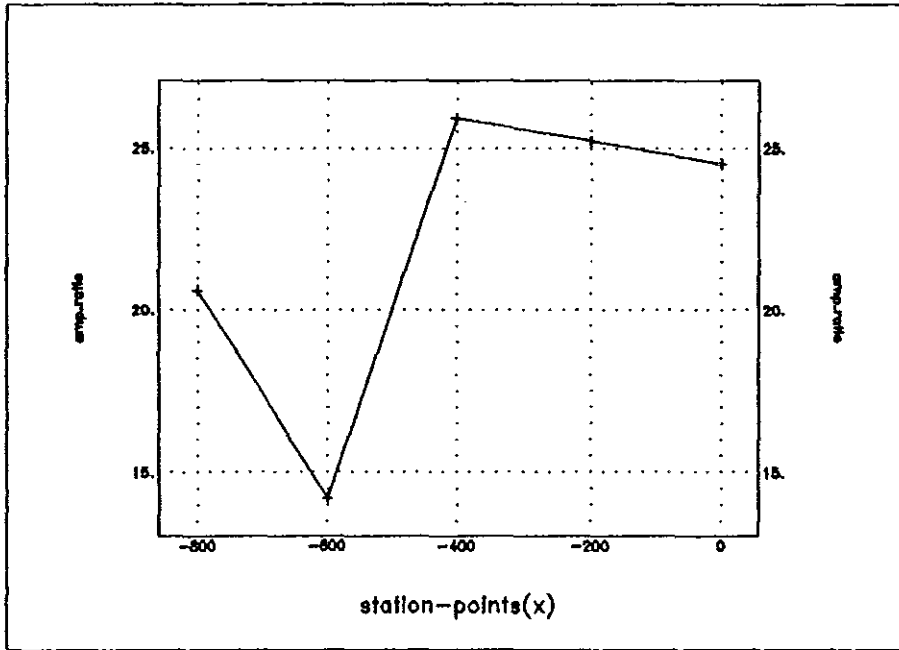


25a

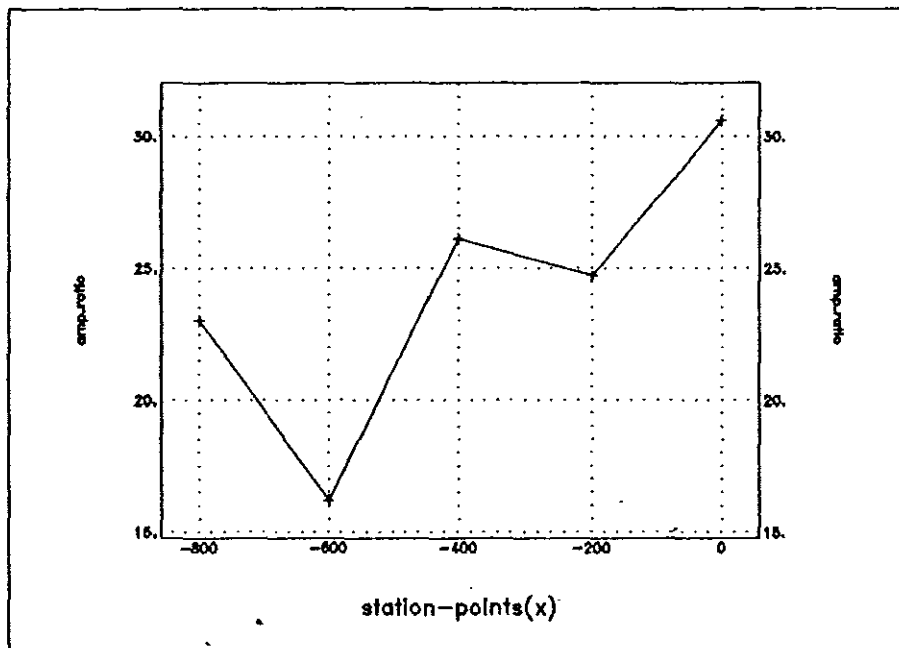


25b

Fig(25a,b) $AB/2=330$

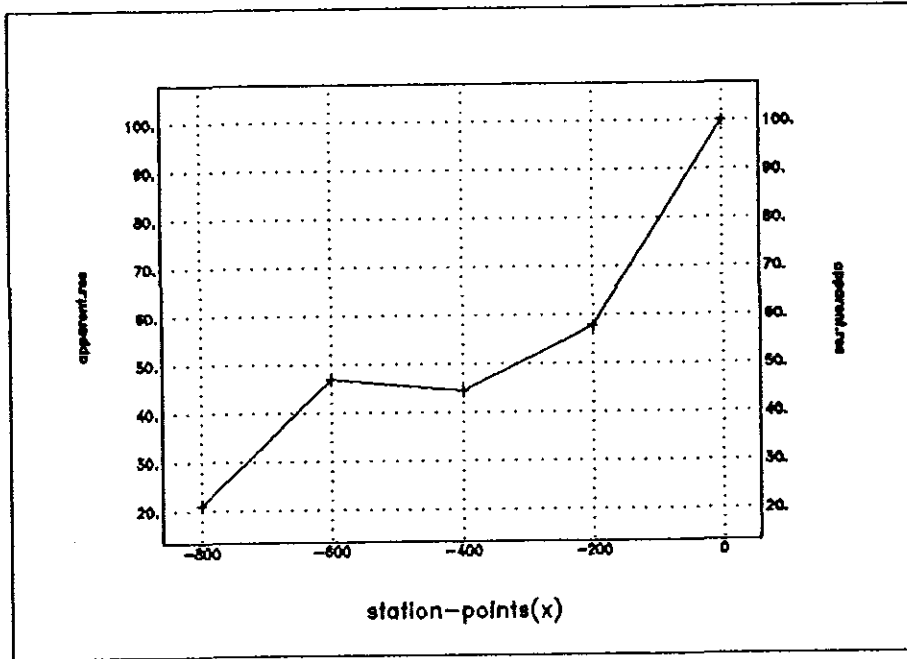


25 c

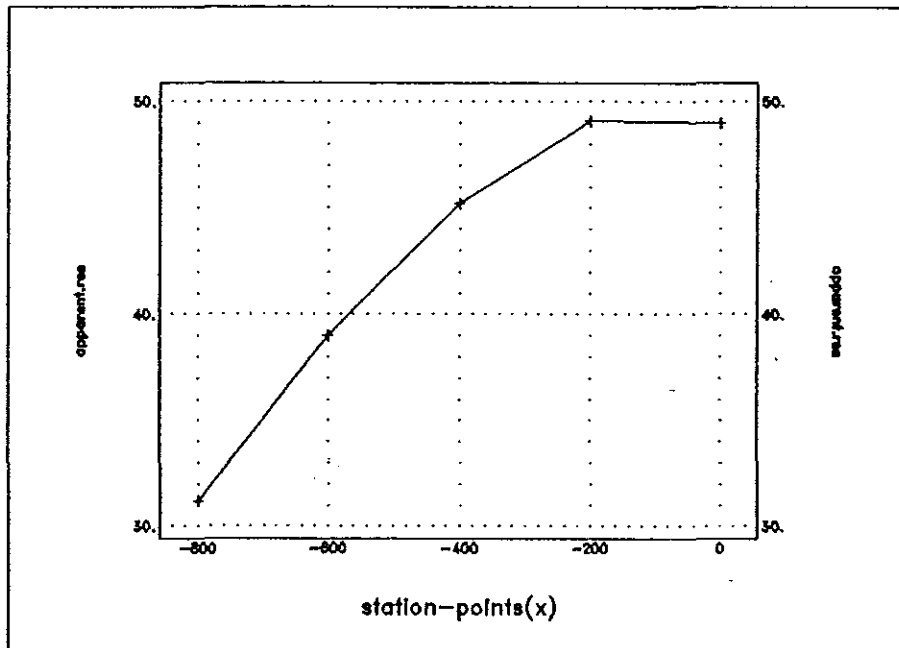


25 d

Fig.(25c)and (d) $\frac{ab}{2}=330$

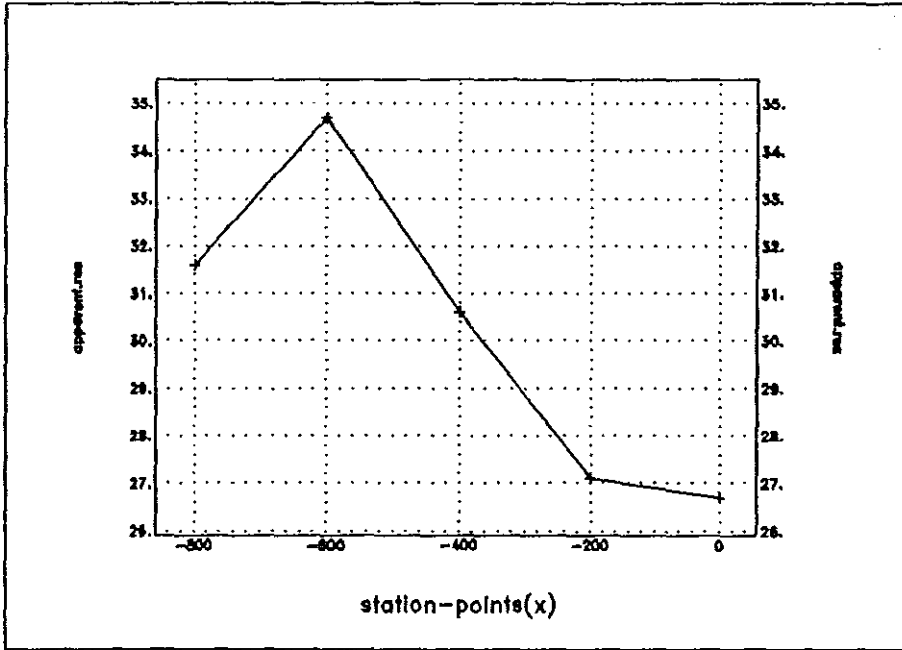


26 a

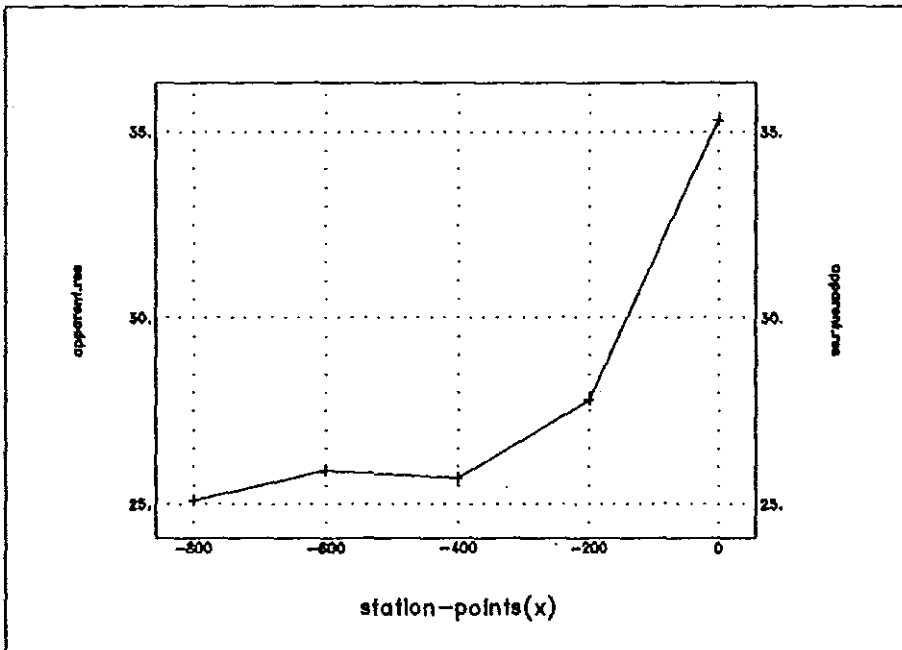


26 b

Fig(26a,b) AB/2=500



26c



26d

Fig.(26c)and (26d) AB=500 profile 3 and 4.

CHAPTER 3

ELECTROMAGNETIC METHOD

GENERAL CONSIDERATIONS

If a time varying electromagnetic field is produced over the ground surface, currents flow in subsurface conductors in accordance with the laws of electromagnetic induction. The currents give rise to secondary electromagnetic (EM) fields which modify the total field observed at any point on the surface. In general the resultant field which may be picked up by a suitable search coil, will differ from the primary field in intensity, phase and direction and would reveal the presence of the conductor.

If the primary field is transient, the secondary currents and their field will decay gradually when the primary field has ceased to exist. The decay is faster when the resistivity of the medium through which the current flows is high. A great advantage of EM methods is that they can be successfully applied even when conductive ground connections which are indispensable for the direct current electrical methods cannot be made owing to highly resistive ground surface conditions. This is frequently the case in arid tracts, in polar and sub polar regions where the ground may be frozen to a considerable depth.

But on the other hand one of the troublesome effects in the EM methods is that the secondary currents in superficial layers of good conductivity (e.g. clays graphitic shales, etc.), may screen the deeper conductors partially or wholly from the primary field. The latter which may be the real objects of explorations, will then produce

weak or no distortions(anomalies) in the total field and may there for be undetectable.(Parasnis, 1976)

3.1 Theory

As the name implies, the method involves, the propagation of time varying, low frequency EM fields, in and over the earth. If this time varying field is produced on the surface of the ground, currents will flow in subsurface conductors in accordance with the laws of electromagnetic induction. These currents will give rise to secondary fields which distort the primary field observed at any point on the surface. In general, the resultant field, which may be picked up by a suitable search coil, will differ in intensity, phase, and direction and reveal the presence of anomalous conductivities in the subsurface. To understand the propagation and attenuation of EM waves, it is important to use Maxwell's equations in a form relating the electric and magnetic field vectors.

$$\vec{\nabla} \times \vec{E} = -\frac{\partial \vec{B}}{\partial t} \quad (20)$$

$$\vec{\nabla} \times \vec{H} = \vec{J} + \frac{\partial \vec{D}}{\partial t} \quad (21)$$

Where, \vec{J} is the current density

\vec{E} is electric field intensity,

\vec{B} is magnetic flux density,

\vec{H} magnetic field intensity and

\vec{D} is electric displacement

Equation (20) is a mathematical statement of Faraday's law which states that an electric field exists in a region of time varying field, such that, the induced electromotive force (emf) is equal to the negative rate of change of magnetic flux.

Equation (21) is a mathematical statement of Ampere's law (taking in to account Maxwell's displacement current $\partial\vec{D}/\partial t$), namely, that a magnetic field is generated in space by current flow and that the field generated is proportional to the total current (both conduction and displacement)

Using the vector identity , $\vec{\nabla} \cdot \vec{\nabla} \times \vec{A} = 0$ for any vector \vec{A} and applying this to the above equations, we get for time varying fields the following relations

$$\vec{\nabla} \cdot \vec{\nabla} \times \vec{E} = -\vec{\nabla} \cdot \frac{\partial \vec{B}}{\partial t} = \frac{\partial (\vec{\nabla} \cdot \vec{B})}{\partial t}$$

or, $\vec{\nabla} \cdot \vec{B} = 0$ (22)

Similarly,

$$\vec{\nabla} \cdot \vec{J} + \vec{\nabla} \cdot \frac{\partial \vec{D}}{\partial t} = \nabla \cdot J + \frac{\partial (\vec{\nabla} \cdot \vec{D})}{\partial t}$$
 (23)

But, we know that the divergence of a current is equivalent to the rate of accumulation of charge and hence,

$$\vec{\nabla} \cdot \vec{J} = \frac{\partial \bar{q}}{\partial t}$$
 (24)

But in regions of finite conductivity, charge doesn't accumulate to any extent during current flow, hence, $\partial q/\partial t = 0$ so that, $\vec{\nabla} \cdot \vec{J}$ vanishes, hence eqn.(23) reduces to:

$$\vec{\nabla} \cdot \vec{D} = 0 \quad (25)$$

Furthermore, in homogenous isotropic media, one can express these relations as,

$$\begin{aligned} \vec{B} &= \mu \vec{H} \\ \vec{D} &= \epsilon \vec{E} \end{aligned} \quad (26)$$

and $\vec{J} = \sigma \vec{E}$

where, σ is electrical conductivity, μ relative permeability and ϵ is dielectric capacity, thus one can simplify equation (20) and (21) using equation (26) as

$$\vec{\nabla} \times \vec{E} = -\mu \frac{\partial \vec{H}}{\partial t} \quad (27)$$

$$\vec{\nabla} \times \vec{H} = \sigma \vec{E} + \epsilon \frac{\partial \vec{E}}{\partial t} \quad (28)$$

using the following vector identity which is valid for rectangular coordinate's only,

$$\vec{\nabla} \times \vec{\nabla} \times \vec{A} = \vec{\nabla}(\vec{\nabla} \cdot \vec{A}) - (\vec{\nabla} \cdot \vec{\nabla} \vec{A}) = \vec{\nabla}(\vec{\nabla} \cdot \vec{A}) - \vec{\nabla}^2 \vec{A} \quad (29)$$

Taking curl of (27) and the above identity, we get ,

$$\vec{\nabla}^2 \vec{E} = \mu \frac{\partial}{\partial t} (\vec{\nabla} \times \vec{H}) , \text{ substituting(28) yields}$$

$$\vec{\nabla}^2 \vec{E} = \mu \frac{\partial}{\partial t} \left(\sigma \vec{E} + \epsilon \frac{\partial \vec{E}}{\partial t} \right)$$

or rearranging ,

$$\vec{\nabla}^2 \vec{E} = \mu \sigma \frac{\partial \vec{E}}{\partial t} + \mu \epsilon \frac{\partial^2 \vec{E}}{\partial t^2} \quad (30)$$

similarly,

$$\begin{aligned}\vec{\nabla}^2 \vec{H} &= -\sigma(\vec{\nabla} \times \vec{E}) - \epsilon \frac{\partial}{\partial t} (\vec{\nabla} \times \vec{E}) \\ \vec{\nabla}^2 \vec{H} &= \mu\sigma \frac{\partial \vec{H}}{\partial t} + \mu\epsilon \frac{\partial^2 \vec{H}}{\partial t^2}\end{aligned}\quad (31)$$

Equations (30) and (31) can be written as

$$\vec{\nabla}^2 \begin{pmatrix} \vec{E} \\ \vec{H} \end{pmatrix} = \mu\sigma \frac{\partial}{\partial t} \begin{pmatrix} \vec{E} \\ \vec{H} \end{pmatrix} + \mu\epsilon \frac{\partial^2}{\partial t^2} \begin{pmatrix} \vec{E} \\ \vec{H} \end{pmatrix}\quad (32)$$

If one chooses time variations which are sinusoidal as,

$$\vec{E}(t) = \vec{E}_0 e^{j\omega t} \quad \text{and} \quad \vec{H}(t) = \vec{H}_0 e^{j\omega t}\quad (33)$$

where $\omega = 2\pi f$ is angular frequency of the field,

Taking the derivatives of Eqn.(33),

$$\begin{aligned}\frac{\partial \vec{E}}{\partial t} &= j\omega \vec{E}, \quad \frac{\partial^2 \vec{E}}{\partial t^2} = -\omega^2 \vec{E} \\ \frac{\partial \vec{H}}{\partial t} &= j\omega \vec{H}, \quad \frac{\partial^2 \vec{H}}{\partial t^2} = -\omega^2 \vec{H}\end{aligned}\quad (34)$$

using (34), eqn(32), reduces to

$$\vec{\nabla}^2 \begin{pmatrix} \vec{E} \\ \vec{H} \end{pmatrix} = j\omega\mu\sigma \frac{\partial}{\partial t} \begin{pmatrix} \vec{E} \\ \vec{H} \end{pmatrix} + \omega^2 \mu\epsilon \begin{pmatrix} \vec{E} \\ \vec{H} \end{pmatrix}\quad (35)$$

Equation(36) is the electromagnetic wave equation for the propagation of electric and magnetic field vectors in an isotropic homogenous medium having electrical conductivity σ , relative permeability μ , and dielectric capacity ϵ .

3.2 DESCRIPTION OF EM FIELDS

General

The primary or source fields used in EM prospecting are normally generated by passing alternating current through long wires or coils. It is essential to know the primary field at the receiver position, or at least to eliminate its effects, because it is always present along with the secondary field due to the currents induced in the subsurface. Consequently, one must measure the disturbing field in the presence of the original primary field (Telford, 1976).

3.2.1 System descriptions

In EM surveys, usually the sources and receivers are wire loops or coils. The form of anomaly depends on system geometry, as well as on the nature of the ground conductors. Coils are described as horizontal or vertical according to the plane in which the windings lie. Thus, the axis of "horizontal" coils for example, is vertical. Systems are also characterized by whether receiver and transmitter coils are coplanar, co-axial or orthogonal, and by whether or not the coupling is at a maximum or minimum, for example, orthogonal coils are minimum coupled and hence primary field is not detected coplanar and co-axial coils are maximum coupled since the primary flux from the transmitter lies along the axis of the receiver coil. Such systems are scarcely affected by slight coil misalignments, but because, strong inphase field is detected even in the absence of a conductor, they are very sensitive to change in coil separation.

3.2.2 Depth of penetration

The question how deep electromagnetic waves penetrate the ground is of great importance in geophysics. If the ground is perfectly insulating the waves could penetrate to any distance. However, owing to the finite conductivity of most surface formations and of the underlying beds, the incident energy is absorbed and amplitudes of the waves decrease exponentially in traversing the conductors due to absorption alone in addition there will be also geometric decrease as the wave spreads. There is also an important parameter which is known as skin depth which describes the depth at which the wave amplitude reduces by $1/e$ of the value at the surface. The general relation is,

$$Z_s = 500 \sqrt{\frac{\rho}{f}} \quad (36)$$

This equation shows skin depth variation with frequency and ground resistivity. This means the higher the resistivity of the ground, the deeper the EM waves propagate and the same is true for lower frequencies. Therefore, EM method has a higher depth of penetration when the resistivity is high and the frequency employed is low.

3.3 EM FIELD PROCEDURES

The standard field procedure is profiling along straight lines. Except in some reconnaissance work, the surveying is done across geologic strike with the line and station spacing dictated by the amount of detail required.

The EM method may be used for vertical drilling in a manner similar to resistivity sounding. This can be accomplished either by increasing the transmitter receiver separation while maintaining constant frequency or by varying the frequency with

components of the secondary field ,generally in percent of the primary field intensity and phase at the receiver coil .The depth of penetration is inevitably limited by the portable low power transmitter. Maximum depth for detecting a good conductor is half the coil spacing, there would be no advantage, however, in increasing the separation beyond 400ft,because the depth would not increase correspondingly(Telford. 1976).

3.3.2 GENIE

This system, like any EM systems consists of measuring variations in the components of electromagnetic fields that are induced by the EM transmitter. The transmitter generates an electromagnetic moment sufficient to energize the ground and penetrate conductive bodies that may be present. Current usually flows through a conductor, such as massive sulfide body or anomalously conductive mineralized body in response to the primary field emanating from the transmitter, in planes that are perpendicular to the lines of the primary field, unless restricted by conductor geometry.

The GENIE mode measures the amplitude of the vertical magnetic fields at two frequencies .The higher frequency (f_2) is the signal frequency and the lower one (f_1) is the reference frequency the receiver computes and displays,

$$\%ratio = \left(\frac{Amp\ 1}{Amp\ 2} - 1 \right) \times 100 \quad (37)$$

where, Amp1 is amplitude of the vertical magnetic field at reference frequency f_1 , Amp2 is amplitude of the vertical magnetic field at signal frequency f_2 .

In an area with no conductors or conductive over burden the GENIE mode will give a reading of zero percent regardless of the coil separation, transmitter or receiver

orientation. This is because both signal and reference fields behave identically in such environments and explains why the GENIE mode has been labeled "geometry invariant". Over a conductor the GENIE mode will describe an anomaly very similar in shape to that seen from the traditional inphase and quadrature HLEM systems. Anomaly behavior with variations in target location, dip, and depth of burial will be much the same for both systems. Fig.(27)

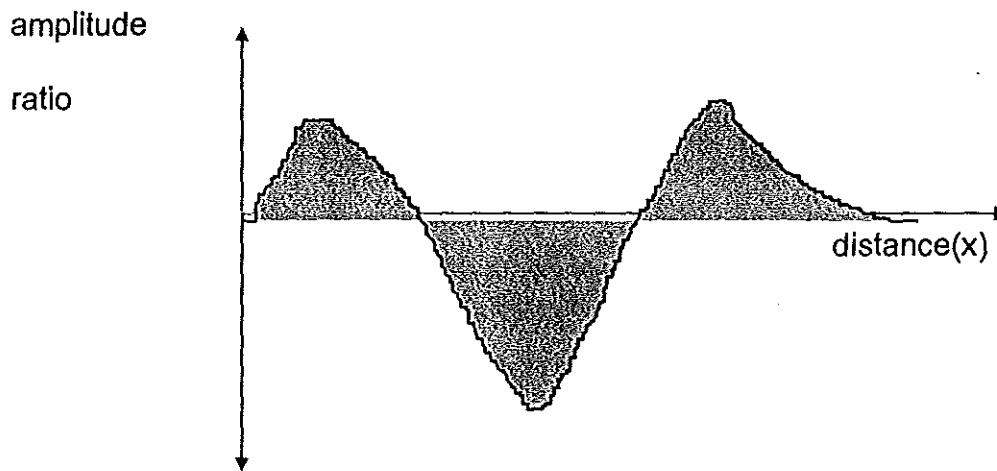


Fig.(27) Typical GENIE response profile

In genie measurements, transmitter and receiver coils are held in horizontal and coplanar geometry as with the conventional horizontal loop(HLEM) systems. The method has been used in place of HLEM systems in areas of moderate to rough terrain for conductors at shallow to moderate depths as it is relatively insensitive to errors in coil positions and orientations

Receiver

The IGS-2/EM4 receiver when used with appropriate transmitter is designed primarily for use in mineral prospecting for massive sulfide ore bodies. It may also be used for the detection of faults or shear zones and to give information about subsurface conductivity for geological mapping ,sand and gravel or ground water

exploration or other geotechnical purposes. the receiver is an EM sensor capable of making amplitude ratio and inphase / quadrature measurements over several pairs of frequencies .

Transmitter

The TM-2 transmitter contains two iron cored coils permitting a pair of frequencies to be transmitted simultaneously. Five frequency pairs between 112.5 and 3137.5 Hz can be selected to cover a broad range of earth conductivity's. Both transmitted signals are derived from crystal controlled master oscillator by variable frequency divisions. The series tuned solenoid in each channel is driven by high efficiency switching amplifier and forms part of two feed back loops. For horizontal loop operation, a signal carrying phase information is generated and sent to the receiver via externally designed isolation transformer and a transmitter receiver interconnecting cable (TM-2 operation manual).

3.4 DATA ACQUISITION

Because the results of EM, survey was intended to supplement some information about the subsurface conductivity for the results obtained from resistivity prospecting method employed in the area, GENIE survey is conducted on the same profile which is used for resistivity sounding. Therefore, for detection of conductive zones the survey was conducted over four parallel profiles which are separated 500 m with each other and extending NW-SE direction. Measurements were taken every 25m-station separation. Two transmitter receiver separations of 50m and 100 m are used and stations along each profile were recorded. It was planned to study the anomaly behavior at two different frequency pairs of 337/112

and 1012/337 but due to technical problems during down loading the data from the console some data for 1012/337 was erased from the memory of the instrument for two profiles.

3.5 Field results

Data processing and presentation

- The collected field data is loaded to the computer and the data is analyzed by geosoft mapping and processing system. In the processing stage two basic processes are conducted.

3.5.1. Profile plotting

In this case, the percent amplitude ratios of vertical magnetic fields were plotted on vertical axis against pickets on the horizontal axis for all the four profiles and the two different frequency pairs which were used for the survey. And GENIE response profiles for both separations and frequency pairs was studied.

3.5.2. Response Contours

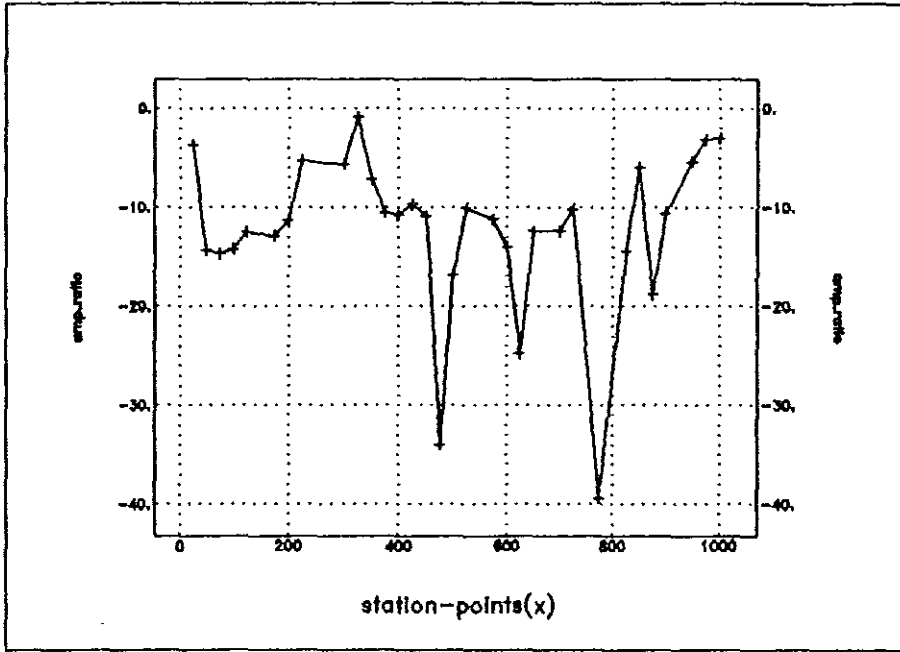
In this case, the collected amplitude ratio over the survey area is contoured so as to study the spatial distribution of conductivity over the area for both transmitter-receiver spacing which were employed for the data collection. From the contours generated for the GENIE responses some additional qualitative over view of earth responses were possible. By analyzing the response profile and contours the researcher was able to gain an intuitive felling for the nature of the conductors giving rise to his observed field responses.

3.6 DATA INTERPRETATION

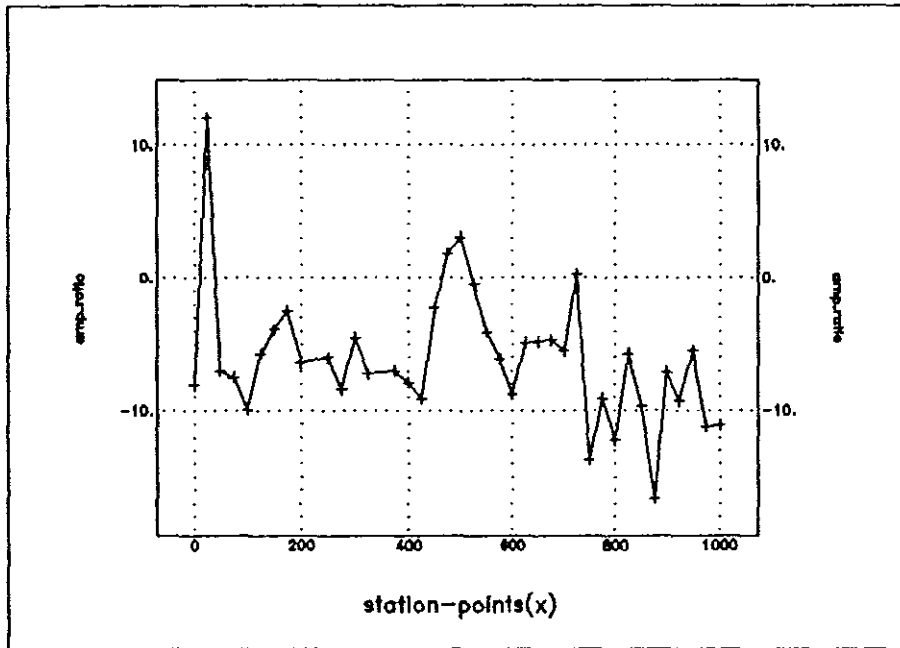
As we can see on the Fig.(28) the response corresponding to the fourth profile, it is possible to see negative GENIE responses depicting high conductivity of the area .This area is described by low apparent resistivity by the resistivity survey of the previous chapter. This high conductivity value is observed all along the profile attaining the highest value at 800 w this anomalously high conductivity value of the area is also clearly shown for the response profile generated for transmitter receiver separation of 50 m. This negative GENIE response detected over this zone could be attributed to clay, the anomaly detected has two distinct maximum negative amplitudes at 475 and 775 W which may correspond to high saturation of the places.

From the response corresponding to the third profile Fig(29). It is also observable that negative amplitude ratios persist all through out the profile with an increasing negative values which may be attributed to the trend of increasing conductivities to wards the western profile. This is also in good confirmation with lower resistivity result obtained in the resistivity survey.

The analysis of the response corresponding to the second profile shows higher amplitude ratio values Fig(30). Which shows the resistive nature of the zone as compared with the fourth and the third profiles. Some anomalously high negative value of GENIE response is detected at the location of 200 W flanked by two positive peaks at each side. This may correspond to the saturation of the area. This peak value is also observed on both TX-RX separations but is more pronounced on the larger spacing. The GENIE response profile for (1012/337) also shows a decreasing response

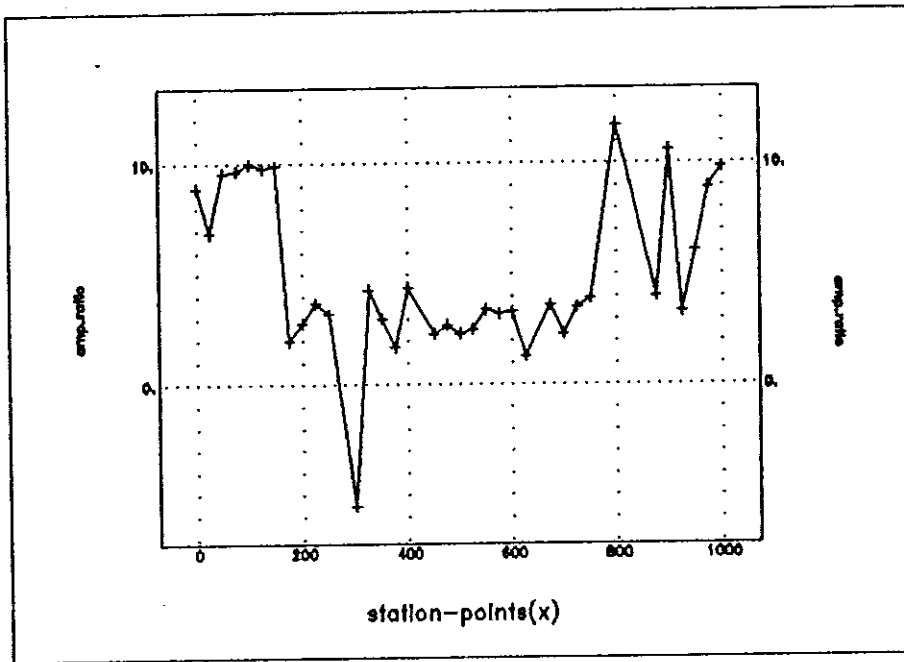


28

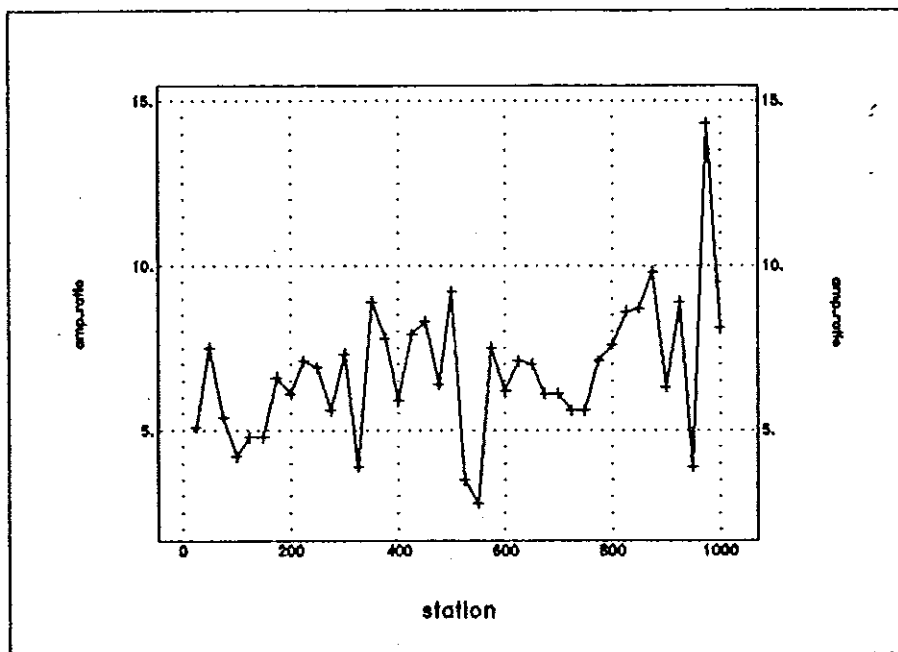


29

Fig.(28) and (29)



30



31

Fig.(30),(31)

function towards the western profile which suggests an increasing conductivity of the ground along this direction.

The GENIE response of the first profile Fig.(31) is described by non negative amplitude ratio peaks suggesting that the zone is some what resistive this could be discussed in light of the shallowness of the bed rock which was observed by the resistivity survey.

Contours

From the amplitude ratio of the Genie response contour It was also possible to observe conductivity variations over the surveyed area. The fourth and the third profile, are described by high conductivity zones describing the higher degree of saturation of this zone. Except the three anomalously conductive zones located at stations (475), (625), and (800) the area is uniformly conductive all along the profile. The middle part of the graph suggests intermediate conductivity values as we see it along the second profile. The contour also shows lower conductivity values for regions around the first profile which is observed also on the Genie response profile plot and resistivity surveys. Fig(32) and (33)

EM RESPONSE CONTOUR MAP

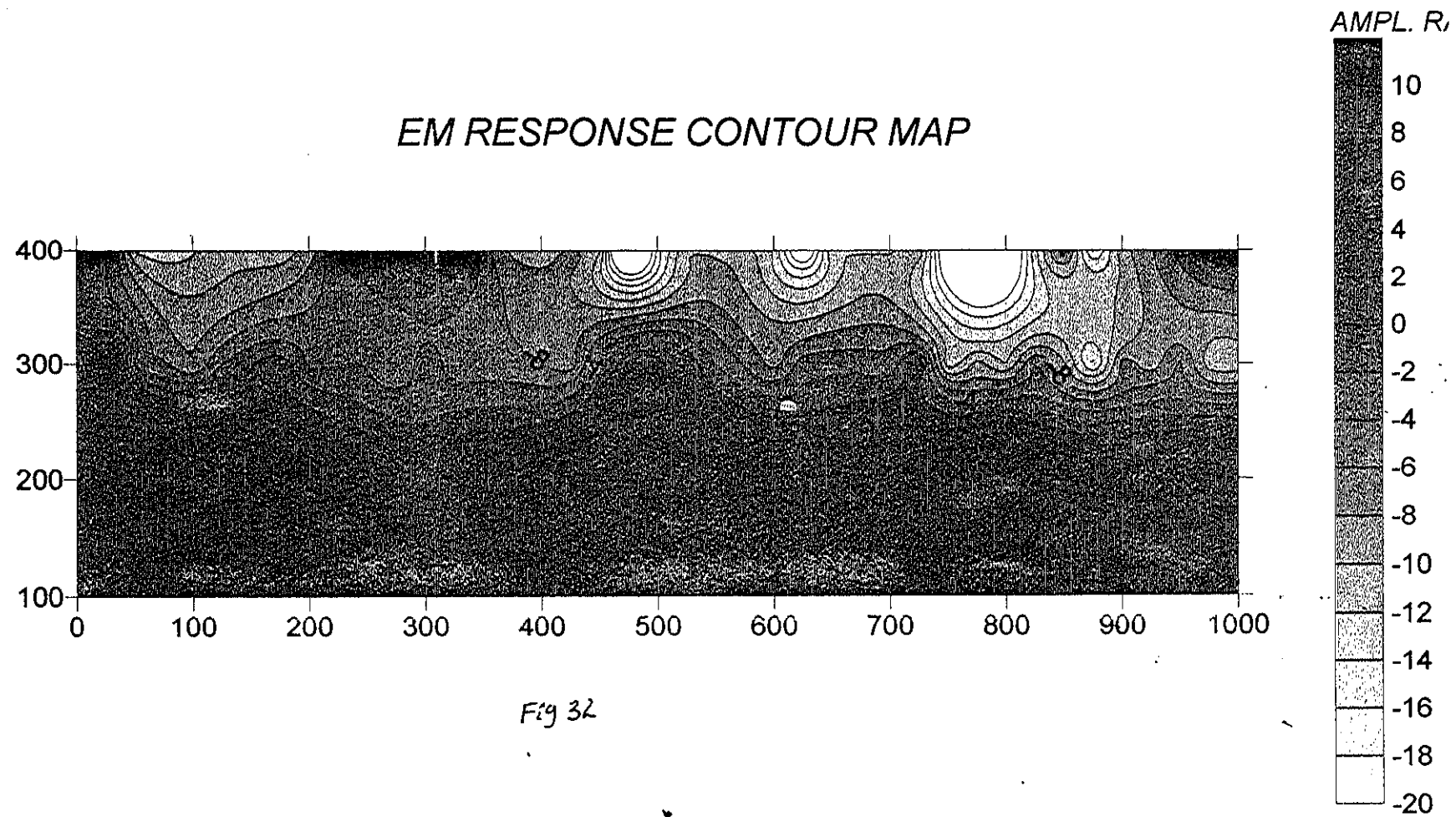


Fig 32

87

89

EM RESPONSE CONTOUR MAP

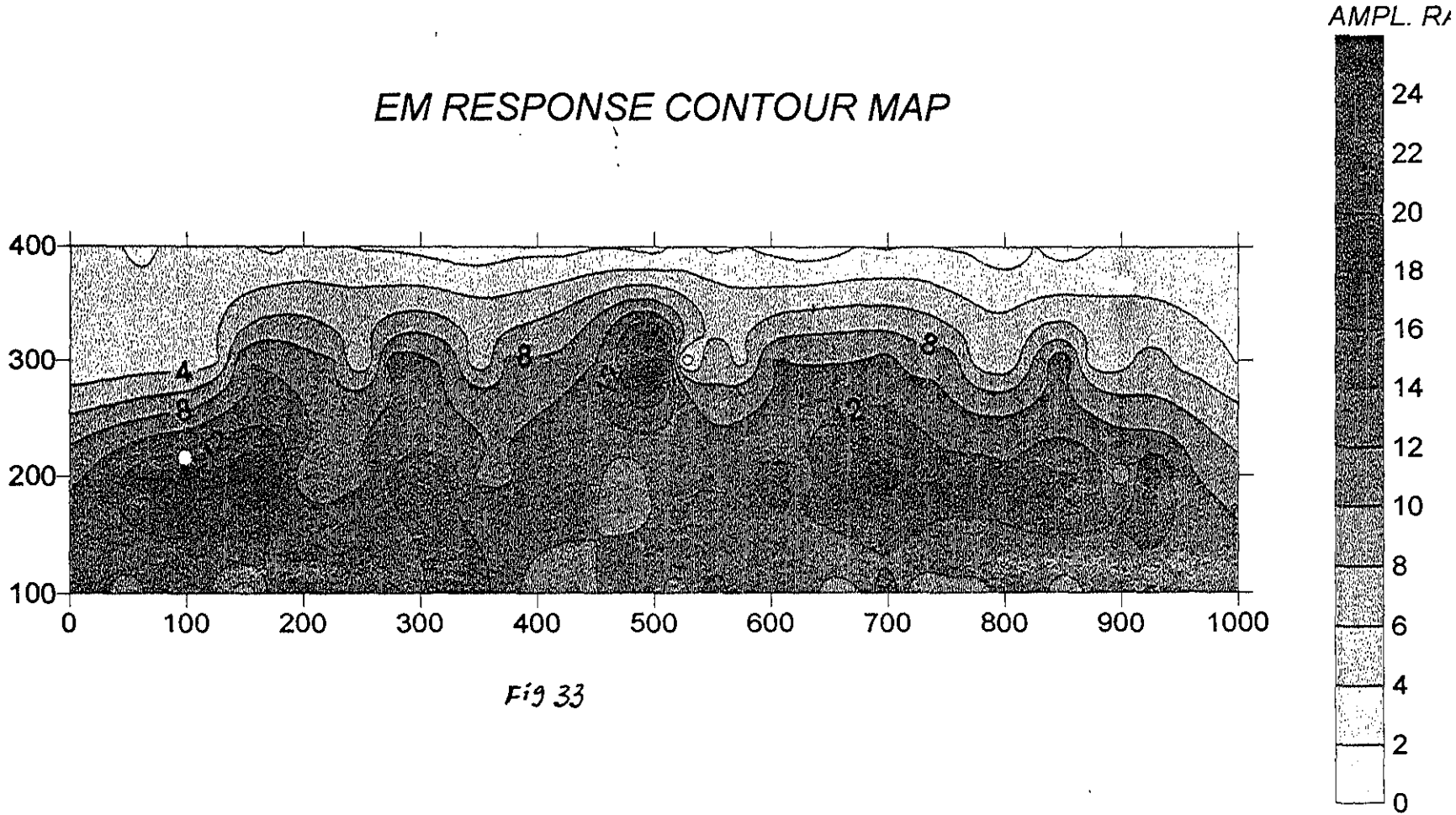


Fig 33

CHAPTER FOUR

SUMMARY AND CONCLUSIONS

Two geophysical methods, namely, vertical electrical sounding (VES) and GENIE electromagnetic prospecting methods were employed at Dembi area near Debrezeit town.

The resistivity survey conducted in this area was Schlumberger expanding spread. The results obtained from vertical electrical soundings were interpreted based on geoelectric sections, pseudo sections, apparent resistivity contours and profile plots which gave important results about both layer stratification and lateral electrical property variations in the area.

The geologic situation of the area has been inferred by comparison of the field results of the survey with the available geological and bore hole information from existing wells in adjacent regions. The results of the sounding survey were presented in the form of geoelectric sections which indicated the distribution of layer resistivities and thicknesses, and most of the quantitative interpretations were based on these sections. More over, the apparent resistivity values were presented in the form of pseudosections and apparent resistivity contour maps, which qualitatively showed the vertical and lateral variations of electrical properties with in the sub surface.

A four layer geoelectric section was constructed based on VES data over the investigated area. On all the resistivity sections constructed along the four profiles it was possible to make the following concluding remarks about the geological set up of the studied area.

References

- Dobrin, (1976) Introduction to geophysical prospecting
- M.Dorn. (1985) A special aspect of interpretation of geo-electric sounding curves and its application for ground water exploration.
Geophysics V23, No.4 pp 455-70
- Frolich. R.K. (1967) The depth of penetration of dipole arrays as compared with Schullumberger arrangement Geo exp. v5. N3. pp72-281
- Genie E.M. Manual,(1988) Scintrex limited Concord, Ontario, Canada.
- Igzaw Solomon, (1974), Short report on Hydrogeology of Debrezeit Area
Eth. Inst. Geol. Survey A.A.
- In man, J.R. Ryu, J. And Ward,S.h. (1973) Resistivity inversion in Geophysics
V40, P 798-817
- M. Israel, (1994) Resistivity data interpretation for the identification of subsurface electrical structure of the earth. Physics education April -
June 1994 pp 25-35
- Kashef,A.A.I, Ground water Engineering. McGraw-hi11 Inc.NY.
(1986)
- Mohr,P.A. (1961) The Geological origin and structure of Bishoftu explosion Crators.
Bull.Geop.Obse. Vo, No2, A.A
- Mohr,P.A (1967) The Ethiopia Rift System.Bull.Geo..Obse.VII A.A
- Marquardt, D.W.(1963) Generalized inverses, ridge regression biased
non linear estimation.

- Ronald A. Van Overmeeren, (1980) Combination of electrical resistivity seismic refraction, and gravity measurements for ground water exploration in Sudan Geophysics V 46 pp 1304-10314
- Parasnis D.S., (1979) Principles of applied Geophysics. Chapman and Hall. John Wiley and Sons, New York. PP1-69
- Parasnis D.S, (1965) Theory and practice of electric potential and resistivity prospecting using linear current electrodes. Georex V3, No1.
- D. Patella (1978) A proposal of new Geoelectrical method; Theory application and practical implications. Geo. Exp. V16. No3. pp223-235
- Patra and Battacharia, (1966). Geophysical exploration for ground water around Digha, India. Geo-exploration V4 PP 209-218
- A.S. Saydam and Duck Worth (1978) Georex V. 16, No. 4 pp 267-289
- Shimeles Fisseha (1992) Some studies on indirect and direct interpretation of field VES curves. MSC. thesis IIT, Kharagpur. India)
- Telford W.H et al (1976) applied Geophysics- Cambridge University press. Cambridge.
- Tamiru Alemayehu (1992) Hydrogeology of Debrezeit Area MSC- Thesis, Addis Ababa University.
- K. Westerberg, (1965) 'The Beam slingram' a new portable E.M instrument for ore prospecting Geo exp. Vs, No3 PP 149-154.
- Wilson (1995) Field Geophysics, Geological society of London Hand book. John Wiley and Sons.